



Mathematisches  
Forschungsinstitut  
Oberwolfach



# Oberwolfach Preprints

OWP 2015 - 13

LOUIS HIRSCH KAUFFMAN AND  
VASSILY OLEGOVICH MANTUROV

Graphical Constructions for the  $sl(3)$ ,  $C_2$  and  $G_2$   
Invariants for Virtual Knots, Virtual Braids and Free  
Knots

Mathematisches Forschungsinstitut Oberwolfach gGmbH  
Oberwolfach Preprints (OWP) ISSN 1864-7596

## Oberwolfach Preprints (OWP)

Starting in 2007, the MFO publishes a preprint series which mainly contains research results related to a longer stay in Oberwolfach. In particular, this concerns the Research in Pairs-Programme (RiP) and the Oberwolfach-Leibniz-Fellows (OWLF), but this can also include an Oberwolfach Lecture, for example.

A preprint can have a size from 1 - 200 pages, and the MFO will publish it on its website as well as by hard copy. Every RiP group or Oberwolfach-Leibniz-Fellow may receive on request 30 free hard copies (DIN A4, black and white copy) by surface mail.

Of course, the full copy right is left to the authors. The MFO only needs the right to publish it on its website *www.mfo.de* as a documentation of the research work done at the MFO, which you are accepting by sending us your file.

In case of interest, please send a **pdf file** of your preprint by email to *rip@mfo.de* or *owlf@mfo.de*, respectively. The file should be sent to the MFO within 12 months after your stay as RiP or OWLF at the MFO.

There are no requirements for the format of the preprint, except that the introduction should contain a short appreciation and that the paper size (respectively format) should be DIN A4, "letter" or "article".

On the front page of the hard copies, which contains the logo of the MFO, title and authors, we shall add a running number (20XX - XX).

We cordially invite the researchers within the RiP or OWLF programme to make use of this offer and would like to thank you in advance for your cooperation.

## Imprint:

Mathematisches Forschungsinstitut Oberwolfach gGmbH (MFO)  
Schwarzwaldstrasse 9-11  
77709 Oberwolfach-Walke  
Germany

Tel +49 7834 979 50  
Fax +49 7834 979 55  
Email [admin@mfo.de](mailto:admin@mfo.de)  
URL [www.mfo.de](http://www.mfo.de)

The Oberwolfach Preprints (OWP, ISSN 1864-7596) are published by the MFO.  
Copyright of the content is held by the authors.

## Graphical constructions for the $sl(3)$ , $C_2$ and $G_2$ invariants for virtual knots, virtual braids and free knots

Louis Hirsch Kauffman

*Department of Mathematics, Statistics  
and Computer Science (m/c 249),  
University of Illinois at Chicago,  
851 South Morgan Street,  
Chicago, Illinois 60607-7045, USA  
kauffman@uic.edu*

Vassily Olegovich Manturov

*Bauman Moscow State Technical University,  
2nd Baumanskaya St. 5/1, Moscow 105005, Russia  
Laboratory of Quantum Topology,  
Chelyabinsk State University,  
Brat'ev Kashirinykh Street 129,  
Chelyabinsk 454001, Russia  
vomanturov@yandex.ru*

Received 10 July 2014

Accepted 16 April 2015

Published 27 May 2015

### ABSTRACT

We construct graph-valued analogues of the Kuperberg  $sl(3)$  and  $G_2$  invariants for virtual knots. The restriction of the  $sl(3)$  and  $G_2$  invariants for classical knots coincides with the usual Homflypt  $sl(3)$  invariant and  $G_2$  invariants. For virtual knots and graphs these invariants provide new graphical information that allows one to prove minimality theorems and to construct new invariants for free knots (unoriented and unlabeled Gauss codes taken up to abstract Reidemeister moves). A novel feature of this approach is that some knots are of sufficient complexity that they evaluate themselves in the sense that the invariant is the knot itself seen as a combinatorial structure. The paper generalizes these structures to virtual braids and discusses the relationship with the original Penrose bracket for graph colorings.

*Keywords:* Knot; link; virtual knot; graph; invariant; Kuperberg  $sl(3)$  bracket; Kuperberg  $C_2$  bracket; Kuperberg  $G_2$  bracket; quantum invariant.

Mathematics Subject Classification 2010: 57M25, 57M27

## 1. Introduction

This paper studies a generalization of virtual knot theory of the Kuperberg  $sl(3)$  bracket invariant and the Kuperberg  $G_2$  invariant. Kuperberg discovered bracket

state sums that depend upon a reductive graphical procedure similar to the Kauffman bracket. The present paper contains new results and reviews results in [17, 28] putting these results in the more general contexts of minimality, parity, virtual braids and graph coloring. The invariants that we study apply to virtual knots and links, flat virtual knots and links, and free knots and links. Free knots and links are unlabeled Gauss diagrams, taken up to abstract Reidemeister moves, and are fundamental to all aspects of virtual knot theory.

This paper is partially expository, intended to describe both our new work and its background. In particular, we review virtual knot theory and the variants of virtual knot theory that are relevant to our study. Virtual knot theory, at the combinatorial level, is the study of Gauss codes or Gauss diagrams up to Reidemeister moves without the planarity restriction on the codes that gives classical knot theory. Gauss codes are to classical knots as arbitrary graphs are to planar graphs. It is important, in understanding virtual knot theory, to take this analogy to heart. In graph theory it is natural to consider the *genus of a graph*, the least genus of an orientable surface in which the graph can be embedded. Just so, in virtual knot theory, one can ask for the least genus surface in which a particular Gauss code can be embedded as a knot or link diagram. However, since for topological purposes one studies the Gauss code up to Reidemeister moves, the genus of a given diagram may not be the least genus among all possible Reidemeister equivalent codes. The *genus* of a virtual knot is the least genus surface that can support the embedding of some representative code for that knot. Classical knots have genus zero in this sense, and there are virtual knots of all possible values of the genus. Kuperberg [20] proved that for standard virtual knots (corresponding to oriented Gauss codes) the embedding type of the virtual knot in its minimal genus surface is unique up to Reidemeister moves in the surface and orientation preserving homeomorphisms of the surface to itself. In fact one can reformulate the theory of virtual knots and links in terms of stabilized embeddings of collections of circles in orientable surfaces crossed with the unit interval. See Sec. 2 for more details about this reformulation. Nevertheless, the key to virtual knot theory is, from our point of view, to regard it as a generalization of knot theory to a topological theory of Gauss codes. This means that there are a number of variants of the theory, depending upon what structure of Gauss codes one uses. The simplest structure is to regard the code as a finite sequence of symbols, each symbol repeated twice, taken up to cyclic order and using the flat (no over- or under-crossings) version of the Reidemeister moves. This virtual theory is called by us *free knots* and is the combinatorial underpinning of all variants of virtual knot theory. Note that in working with the combination of combinatorics and topology, features of combinatorial representations can become topological invariants if one asks for their minimal appearance in some form. For example, every Gauss code has a least genus surface in which it can be embedded. The least genus among all codes that represents the same topological type

is an invariant of the topological type. Thus each free knot has a minimal genus in this sense. The methods of this paper allow the determination or estimation of this genus by giving irreducible graphs that are part of any representative for the given free knot. One can determine the genus of such irreducible graphs and thereby obtain a lower bound on the genus of the free knot or virtual knot in question.

In this paper we show that the Kuperberg bracket invariants can be uniquely defined and generalized to virtual knot theory. This is accomplished via reductive graphical equations. These equations reduce to scalars only for the planar graphs from classical knots. Thus our new invariants take values in linear combinations of graphs with polynomial coefficients. We will call these “graph polynomials”. The ideal case, sometimes realized, is when the topological object is itself the invariant, due to irreducibility. When this happens one can point to combinatorial features of a topological object that must occur in all of its representatives. This was first pointed out by Manturov in the context of parity. These new invariants specialize to invariants of free knots and allow us to prove that many free knots are non-trivial without using the parity restrictions we had used before.

In [17, 28] we extended the Kuperberg combinatorial construction of the quantum  $sl(3)$  invariant for the case of virtual knots. In [18] the  $sl(3)$  invariant is applied to classical knots using virtuality. In this paper, we shall review this construction, the  $C_2$  construction, and we shall analyze the corresponding construction for the  $G_2$  invariant. In the case of the  $G_2$  construction, we find that this kind of extension works best for free knots. This will be explained in the body of the paper. In speaking of knots in this paper we refer to both knots and links.

In many figures we adopt the usual convention that whenever we give a picture of a relation, we draw only the changing part of it; outside the figure drawn, the diagrams are identical. In Fig. 1 we illustrate the basic expansion relations for the  $sl(3)$  bracket. Note that two sided faces and quadrilaterals are expanded. The oriented graphs that can appear must, due to the orientations imposed, have an even number of edges per face. Planar graphs with only cubic vertices are seen by the Euler formula to have regions with two, three, four or five faces. Since here three and five sided faces are ruled out, we see that in the plane the expansion of the  $sl(3)$  bracket reduces to scalar. We show that for virtual knots, with their underlying non-planar graph structure, this is no longer the case. The invariant generalizes to virtual knots, but takes values in graphs with Laurent polynomial coefficients.

For the case of the  $sl(3)$  knot invariant, one uses the relation shown in Fig. 1, see [19]. This means that the left (respectively, right) picture of Fig. 1 is resolved to a combination of the upper and lower pictures with coefficients indicated on the arrows. The advantage of Kuperberg’s approach is that graphs of this sort which can be drawn on the plane can be easily simplified, by using further linear relations,

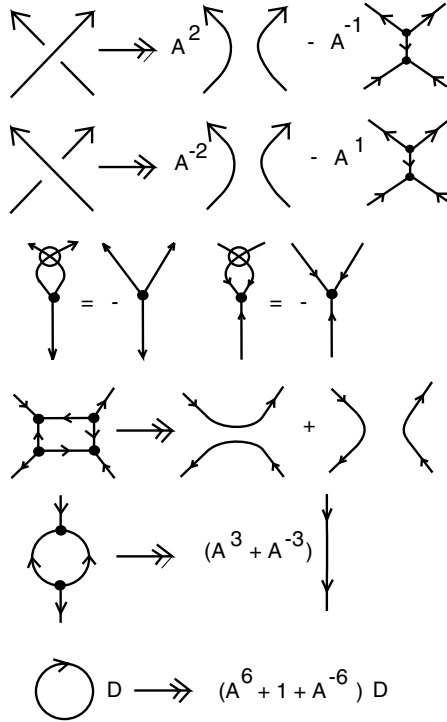


Fig. 1. Kuperberg bracket for  $sl(3)$ .

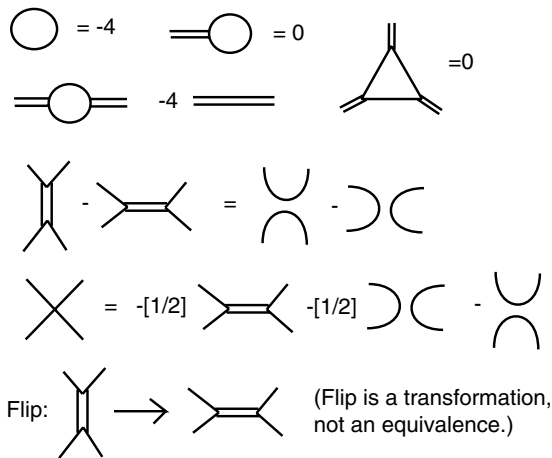


Fig. 2. Kuperberg's relation for  $C_2$ .

to collections of Jordan curves, which in turn, evaluate to elements from  $\mathbb{Z}[A, A^{-1}]$ . For planar graphs, these reductions continue all the way to scalars. In the case of non-planar graphs, some states in the expansion may not contain quadrilaterals or bigons. Such states are irreducible and will receive a possibly non-zero polynomial coefficient in the new invariant. Non-planar resolutions can leave irreducible graphs whose properties reflect the topology of virtual knots and links. The presence of a single such irreducible graph can guarantee the non-triviality and non-classicality of a virtual knot or a free knot. The oriented structure of the states of the  $sl(3)$  invariant makes it possible to sometimes reconstruct the knot from one of its states, but such reconstruction is not guaranteed.

A triangle is *bad* if it has a vertex with two outgoing edges; a quadrilateral is bad if it has two vertices each having two outgoing edges. The  $sl(3)$  invariant yields the minimality of those oriented framed 4-regular graphs that have no bad triangles and no bad quadrilaterals.

See Fig. 2 for the expansion patterns for the  $C_2$  invariant. Here there are single and double lines in the unoriented graphs, and a graph with a maximal number of double lines can be sometimes used to decode the original knot. In the case of this expansion, one obtains an invariant of free knots.

The main subject of this paper is an extension of the Kuperberg  $G_2$  invariant to an invariant of free knots. See Fig. 3 for the expansion formula for this invariant, Fig. 4 for the loop, triangle and square relations, and Fig. 5 for the pentagon relation. Once again, this invariant can detect free knots when there are irreducible states.

This paper is organized as follows. Section 2 introduces the basics of virtual knot theory including definitions of flat knots and free knots. Section 3 discusses parity and the parity bracket. Section 4 contains the construction of the  $sl(3)$  invariant for virtual knots, flat knots and free knots and the construction of the  $G_2$  invariant for flat knots and free knots. Section 5 discusses minimality theorems and modes of detection of knottedness using these invariants. Section 6 gives a small collection of specific examples. Section 7 is a discussion of the Penrose coloring bracket, showing that it is a specialization of the  $sl(3)$  invariant. It is worth putting the Penrose bracket in this context since it can be regarded as the precursor of all these

$$\begin{array}{c}
 \begin{array}{c} \diagup \diagdown \\ \diagdown \diagup \end{array} = a \begin{array}{c} \cup \\ \cap \end{array} + b \begin{array}{c} \cup \\ \cap \end{array} + c \begin{array}{c} \diagup \diagdown \\ \diagdown \diagup \end{array} + d \begin{array}{c} \diagup \diagdown \\ \diagdown \diagup \end{array} \\
 a = q/(1+1/q) \quad c = 1/(1+q) \\
 b = (1/q)/(1+q) \quad d = 1/(1 + 1/q) \\
 q=1: a=b=c=d =1/2
 \end{array}$$

Fig. 3.  $G_2$  crossing expansion.

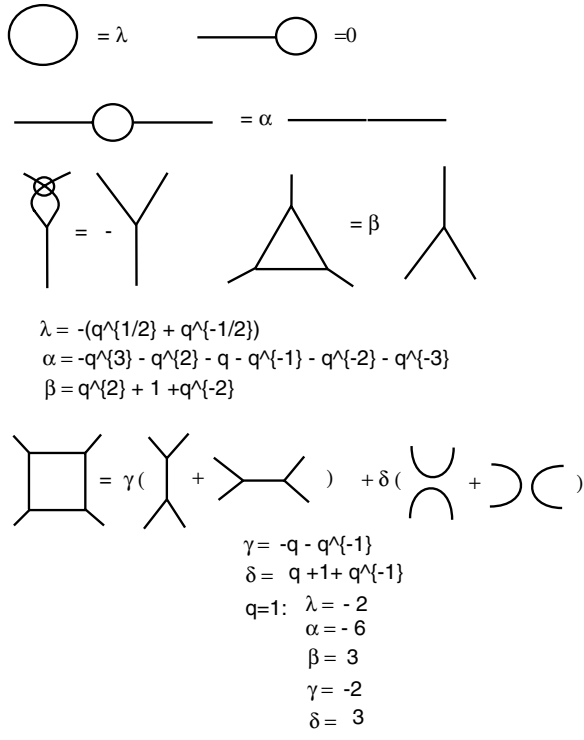


Fig. 4. Loop, triangle and square relations for the  $G_2$  bracket.

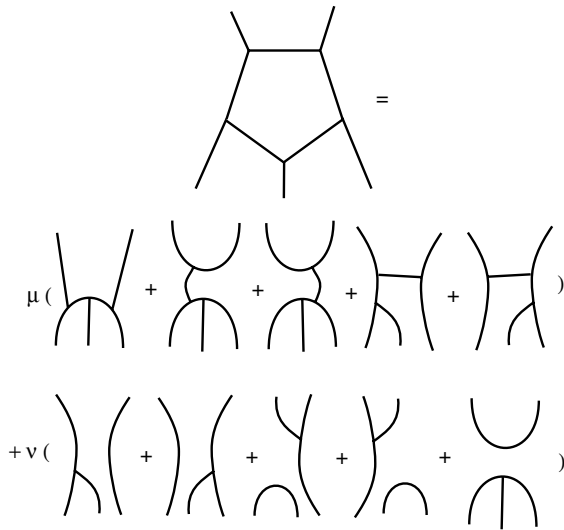


Fig. 5. Pentagon relation for the  $G_2$  bracket.



invariants, and because it is a significant state sum for counting colorings of planar trivalent graphs. Section 8 contains closing remarks.

## 2. Basics of Virtual Knot Theory, Flat Knots and Free Knots

This section contains a summary of definitions and concepts in virtual knot theory that will be used in the rest of the paper.

In classical knot theory, one studies the (isotopy classes of) embeddings of disjoint collections of oriented circles into the three-dimensional sphere or into a chosen three-dimensional manifold. Thus classical knot theory is concerned with the placement problem for circles in three-manifolds. For knots and links in the three-sphere or Euclidean three-space, one can project the knot generically to the surface of a two-dimensional sphere so that the only singularities are transverse double points. This projection, with extra information at the double points to indicate the relative height of the projection, is called the *link diagram*. It is a locally four-valent graph in the two-sphere with the above extra structure at the nodes (crossings). The *Gauss code* of a diagram is obtained by walking along a component of the diagram and recording at each crossing  $i$  whether the walk takes you over or under the crossing and what is the sign of the crossing. Thus  $O_i+$  records that the crossing  $i$  is traversed over and that the crossing itself is positive. See Fig. 8 for an illustration of the trefoil knot with Gauss code  $T = O_1 + U_2 + O_3 + U_1 + O_2 + U_3 +$ . The convention for crossing signs should be apparent from the figure: a crossing is *positive* if a counterclockwise turn of the overdressing segment brings it into coincidence with the orientation of the under-crossing segment. Otherwise the crossing is *negative*. Note that each crossing appears twice in the Gauss code. A knot code such as  $T$  above is taken up to cyclic order for a given diagram. For links one needs one such cyclic code for each component of the link. Along with the Gauss code it is convenient to have *Gauss diagrams*. In Fig. 8, we illustrate the Gauss diagram for the trefoil. The Gauss diagram is a combinatorial representation of the Gauss code. It consists in a circle with  $2n$  points for a knot diagram with  $n$  crossings. Each point on the circle appears twice in the order in which it appears in the Gauss code. Points representing the same crossing in the knot diagram are connected by an edge interior to the circle that we refer to as a *chord*. The chords are not necessarily chords of the circle in the classical geometric sense, but one often draws them in that fashion. Then an arrow is placed on each chord to indicate the over/under information for the corresponding crossing. The convention is that as you walk along the circle of the Gauss diagram you will encounter an arrow pointing away from you if you are going over the crossing and an arrow pointing toward you if you are going under the crossing. Each chord is labeled plus (+) or minus (-) according as the corresponding crossing is positive or negative. The Gauss diagram is very useful for handling combinatorial and computational issues about knot diagrams. Again the generalization of links involves more circles and chords between different circles.

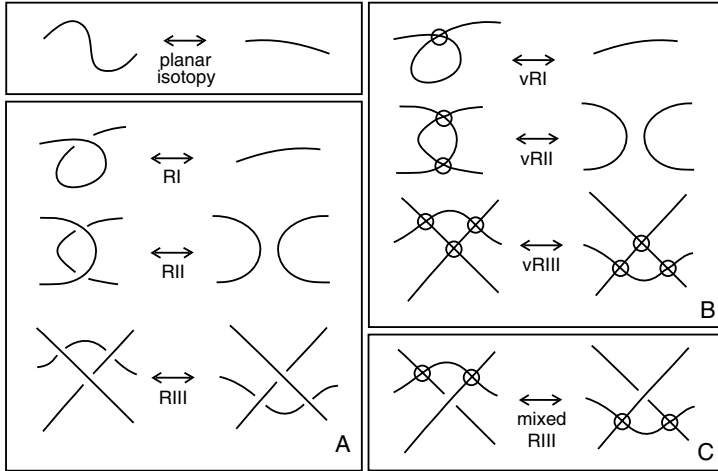


Fig. 6. Moves.

Classical knot theory can be formulated entirely in terms of the knot and link diagrams via the Reidemeister moves [33] depicted in the left-hand half of Fig. 6. These are local replacement moves on the diagrams that each correspond to (elementary) ambient isotopies of the corresponding embedding in three-dimensional space. Two circles embedded in three-dimensional space with corresponding knot diagrams  $K$  and  $K'$  are ambient isotopic in three dimensions if and only if the diagrams  $K$  and  $K'$  can be transformed one to the other by planar isotopy coupled with a finite sequence of the moves  $RI, RII, RIII$  of Fig. 6. Furthermore, one can translate the Reidemeister moves to combinatorial moves on the Gauss diagrams. We omit the details for this translation and simply state that *classical knot theory is equivalent to the theory of planar Gauss codes (or Gauss diagrams) taken up to Reidemeister moves on these codes*. In Fig. 10 we show the Gauss diagram versions of the Reidemeister moves where no restrictions are made for the crossing structure or the orientations. This is the minimal abstract combinatorial structure for the Reidemeister moves and we will return to this structure below. The reader who wants to see the exact Reidemeister moves for Gauss diagrams of classical knots can take on the exercise of adding the correct signs and arrows to the diagrams in this figure.

**Definition 1.** *Virtual Knot Theory (VKT)* is the study of arbitrary oriented Gauss codes (Gauss diagrams) taken up to the equivalence relation generated by the Reidemeister moves on these codes. Two virtual knots or links, represented as such codes, are said to be *virtually isotopic* if one can be obtained from the other by a sequence of Reidemeister moves.

Virtual knots and links can be represented by planar diagrams with extra *virtual crossings* just as non-planar graphs can be drawn in the plane by using

extra crossings. In the diagrammatic theory of virtual knots one adds a *virtual crossing* (see Fig. 6) that is neither an over-crossing nor an under-crossing. A virtual crossing is represented by two crossing segments with a small circle placed around the crossing point. In Fig. 9 we illustrate a virtual knot with Gauss code  $g = O1 + U2 + O3 - U1 + O2 + U3 -$ . Note that this Gauss code differs from the code for the trefoil knot only in the sign of the third crossing. The figure shows the virtual diagram with two virtual crossings, the Gauss code and the Gauss diagram. Planar diagrams with virtual crossings are a convenient way to represent virtual knots and links. By adding to the Reidemeister moves the extra moves shown in Fig. 6 we obtain a complete description of virtual knot theory in terms of these planar diagrams. The extra moves in Fig. 6 are moves that involve the virtual crossings. These moves ((B) and (C)) are designed to generate exactly the same relation as the single nonlocal *detour move* of Fig. 7. The detour move allows one

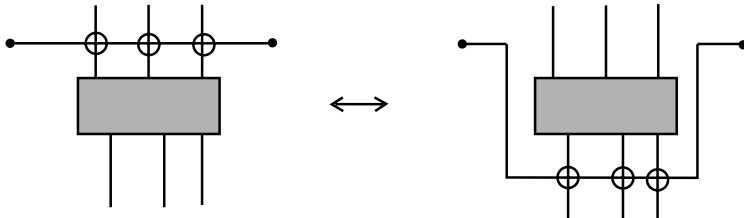


Fig. 7. The detour move.

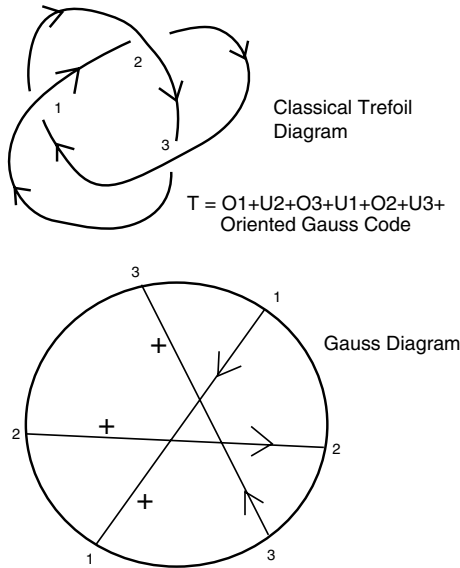


Fig. 8. Gauss code and Gauss diagram for classical trefoil.

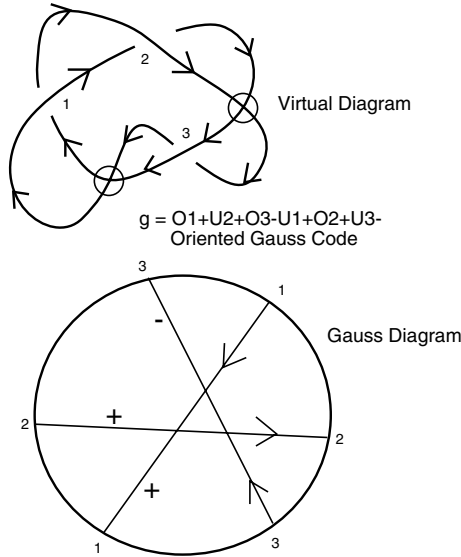


Fig. 9. Gauss code and Gauss diagram for a virtual knot.

to cut away a segment consisting only virtual crossings and to reconnect it in any way on the diagram, again through virtual crossings. Thus the detour move insures that the diagrammatic equivalence relation for virtual knots and links is the same as that given in diagram-free Gauss code definition.

Virtual diagrams can be regarded as representatives for oriented Gauss codes [3, 9, 10] (Gauss diagrams). Such codes do not always have planar realizations. *Virtual isotopy is the same as the equivalence relation generated on the collection of oriented Gauss codes by abstract Reidemeister moves on these codes.* The reader can see this approach in Refs. 3, 13 and 29. It is of interest to know the least number of virtual crossings that can occur in a diagram of a virtual knot or link. If this virtual crossing number is zero, then the link is classical. For some results about estimating virtual crossing number see [2, 14, 26] and see the results of Corollaries 3 and 4. In Sec. 3 we not only count virtual crossings, we count combinatorial substructures of the diagram that may be unavoidable for a given invariant (in a sense that we specify later in the paper). The virtual crossing estimates first achieved in [29] use graphical invariants.

In fact, virtual knot theory studies the embeddings of curves in thickened surfaces of arbitrary genus, up to the addition and removal of empty handles from the surface. See [9, 11]. This is a very fruitful interpretation of virtual knot theory, but we shall not use it in the present paper except in terms of searching for the minimal genus surface in which a virtual knot may be represented.

**Flat Knots and Links.** Every classical knot diagram can be regarded as a 4-regular plane graph with extra structure at the nodes. Let a *flat virtual diagram*

be a diagram with *virtual crossings* as we have described them and *flat crossings* consisting in undecorated nodes of the 4-regular plane graph, retaining the cyclic order at a node. Two flat virtual diagrams are *equivalent* if there is a sequence of generalized flat Reidemeister moves (as illustrated in Fig. 6) taking one to the other. A generalized flat Reidemeister move is any move as shown in Fig. 6 where one ignores the over- or under-crossing structure. The moves for flat virtual knots are obtained by taking Fig. 6 and replacing all the classical crossings by flat (but not virtual) crossings. In studying flat virtuals the rules for transforming only virtual crossings among themselves and the rules for transforming only flat crossings among themselves are identical. Detour moves as in part (C) of Fig. 6 are available for virtual crossings with respect to flat crossings and *not* the other way around.

To each virtual diagram  $K$  there is an associated flat diagram  $F(K)$ , obtained by forgetting the extra structure at the classical crossings in  $K$ . We say that a virtual diagram *overlies* a flat diagram if the virtual diagram is obtained from the flat diagram by choosing a crossing type for each flat crossing in the virtual diagram. If  $K$  and  $K'$  are isotopic as virtual diagrams, then  $F(K)$  and  $F(K')$  are isotopic as flat virtual diagrams. Thus, if we can show that  $F(K)$  is not reducible to a disjoint union of circles, then it will follow that  $K$  is a non-trivial and non-classical virtual link.

**Definition 2.** A *virtual graph* is a 4-regular graph that is immersed in the plane giving a choice of cyclic orders at its nodes. The edges at the nodes are connected according to the abstract definition of the graph and are embedded into the plane so that they intersect transversely. These intersections are taken as virtual crossings and are subject to the detour move just as in virtual link diagrams. We allow circles along with the graphs of any kind in our work with graph theory.

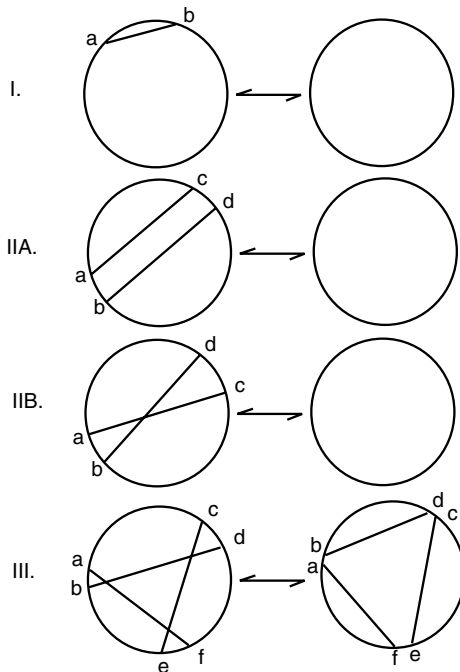
**Framed Nodes and Framed Graphs.** We use the concept of a *framed four-valent node* where we only specify the pairings of *opposite edges* at the node. In the cyclic order, two edges are said to be opposite if they are paired by skipping one edge as one goes around. If the cyclic order of a node is  $[a, b, c, d]$  where these letters label the edges incident to the node, then we say that edges  $a$  and  $c$  are *opposite*, and that edges  $b$  and  $d$  are *opposite*. We can change the cyclic order and keep the opposite relation. For example, in  $[c, b, a, d]$  it is still the case that the opposite pairs are  $a, c$  and  $b, d$ . A *framed four-valent graph* is a four-valent graph where every node is framed. When we represent a framed four-valent graph as an immersion in the plane, we use virtual crossings for the edge-crossings that are artifacts of the immersion and we regard the graph as a virtual graph. For an abstract framed four-valent graph, there are neither classical crossings nor virtual crossings, only the framed nodes and their interconnections.

**Definition 3.** A *component* of a framed graph is obtained by taking a walk on the graph so that the walk contains pairs of opposite edges from every node that is met during the walk. That is, in walking, if you enter a node along a given edge,

then you exit the node along its opposite edge. Such a walk produces a cycle in the graph and such cycles are called the *components* of the framed graph. Since a link diagram or a flat link diagram is a framed graph, we see that the components of this framed graph are identical with the components of the link as identified by the topologist. A framed graph with one component is said to be *unicursal*. A circle with no nodes is considered as a graph; it is a single component.

### 2.1. Free knots

**Definition 4.** *Free knots* are equivalence classes of unoriented, unlabeled Gauss codes with the equivalence relation generated by the abstract Reidemeister moves for Gauss codes, as illustrated in Fig. 10. Figure 12 illustrates a non-trivial free knot and its corresponding virtual diagram. Diagrams for free knots are formed just as we form diagrams for virtual knots and flat virtual knots. However, since we do not make assumptions about cyclic orientation at nodes for the free knot, the virtual diagrams are defined only up to the framing of the classical flat nodes



In all cases there can be many more chords, but no chords intervene between nearby letters in the above diagrams. For example, no chords touch the circle between a and b in I, no chords are between c and d or between a and b in II, and no chords are between a,b or c,d or e, f in III.

Fig. 10. Reidemeister moves on Gauss diagrams.

in the diagram in the sense of the discussion above. This means that the free knots can be modified by interchanging a classical flat crossing with an adjacent virtual crossing as shown in Fig. 11. This interchange is called the  $Z$ -move. Thus *free knots are the same as framed four-valent graphs taken up to the flat Reidemeister moves, and this is the same as flat virtual knots modulo the  $Z$ -move.*

In the  $Z$ -move one can interchange a crossing with an adjacent virtual crossing even in the category of virtual knots and links. We call virtual knots and links modulo the  $Z$ -move,  $Z$ -knots. At this writing we do not know if classical knots and links embed in  $Z$ -knots.

Free knots are the most fundamental combinatorial structure underlying virtual knot theory. If we forget all the structure about a virtual knot except its underlying

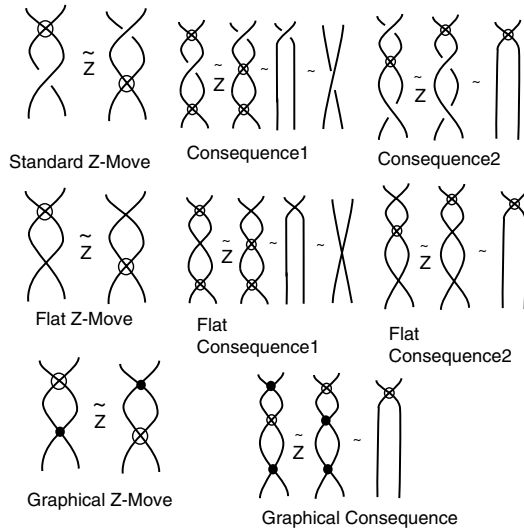


Fig. 11. The  $Z$ -move.

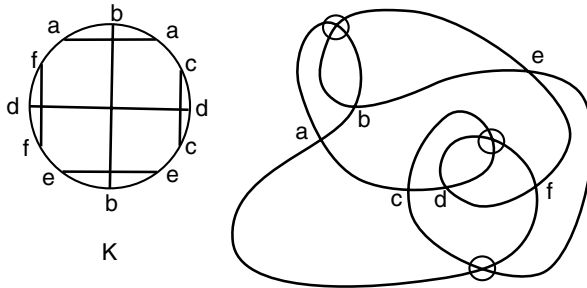


Fig. 12. The free knot  $K$  — Gauss diagram and virtual diagram.

free knot, then the non-triviality of the free knot (if it is non-trivial) will imply that the virtual knot is also non-trivial.

Free knots, implicit as they are in the concept of flat virtuals and Gauss codes, were defined by Turaev [34, 35] sometime after the concepts of virtual knots and flat virtual knots had been articulated. It was not at first obvious that free knots could be non-trivial. In fact, Turaev had conjectured that all free knots were trivial in [35]. A nice breakthrough in understanding this subject was made by Manturov when he discovered the role of parity in identifying non-trivial free knots. View again Fig. 12 and note that every chord has an odd number of intersections with the other chords. As we shall see in the next section, this can be used to show that this is a non-trivial free knot.

Flat knots occupy an intermediate position between virtual knots and free knots. It turns out, however, that flat knots admit a reasonably simple classification and in most of the cases they have a unique minimal (with respect to flat crossing number) diagram, and in most of the cases there is a descending sequence to the minimal diagram. For more details, see [4]. The reason for this simplicity for flat knots is that minimal representatives of flat knots are homotopy classes of curves in a given 2-surface. Virtual knots represent to *isotopy* of curves in three-manifolds (thickened surfaces) which is more complicated than homotopy. We believe that free knots are close to being classified; in the present paper we give yet another invariant which fills some classification gaps. Thus, we draw attention mostly to virtual knots and free knots. Flat and free knots play a very important role for understanding parities and other graphical properties of virtual knots.

### 3. Parity in Knot Theory and Virtual Knot Theory

This section discusses the use of parity in knot theory, virtual knot theory and particularly in the theory of free knots. See [5, 23, 24, 27, 29] for recent work in this area. In this section we discuss the odd writhe of a virtual knot and the Manturov Parity Bracket. The reason for reviewing this material is to recall the parity framework and to illustrate how invariants can sometimes locate irreducible features in diagrams or Gauss codes.

#### 3.1. The odd writhe

**The Odd Writhe  $J(K)$ .** In Fig. 13 we show that the virtual knot  $K$  is not trivial, not classical and not equivalent to its mirror image by computing its *odd writhe* [12]. The odd writhe,  $J(K)$ , is the sum of the signs of the odd crossings. A crossing in a knot diagram is *odd* if it flanks an odd number of symbols in the Gauss code of the diagram. We call this *Gaussian parity* to distinguish it from other parities that can be defined for virtual diagrams. All crossings in a classical knot diagram are even. Hence classical diagrams have zero odd writhe. In the figure, the flat Gauss code for  $K$  is 1212 with both crossings odd. Thus we see that  $J(K) = 2$  for the



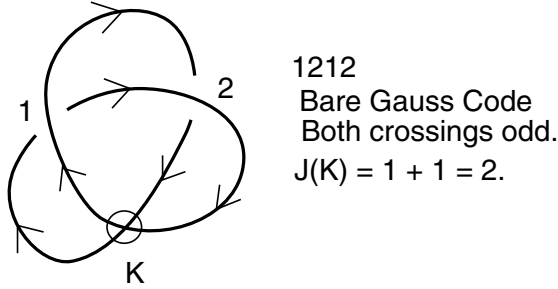


Fig. 13. Example of odd writhe,  $J(K)$ .

knot in the figure. One proves that

- (1)  $J(K)$  is an isotopy invariant of virtual knots,
- (2)  $J(K^*) = -J(K)$  when  $K^*$  is the mirror image of  $K$  (obtained by switching all the crossings),
- (3)  $J(K) = 0$  when  $K$  is isotopic to a classical knot.

The odd writhe is the simplest application of parity in virtual knot theory.

Figure 14 shows why the odd writhe is an invariant of virtual knots by focusing on the third Reidemeister move and the parity of the three crossings involved in that move. We have indicated three crossings by the lowercase letters  $i, j, k$  and have used the capital letters  $I, J, K$  to indicate the number of symbols in the Gauss code between two appearances of the corresponding lowercase letter. The diagram in the figure shows that  $I + J + K$  is necessarily an even number. Thus, either two of the crossings at the third move are odd, or all of the crossings are even.

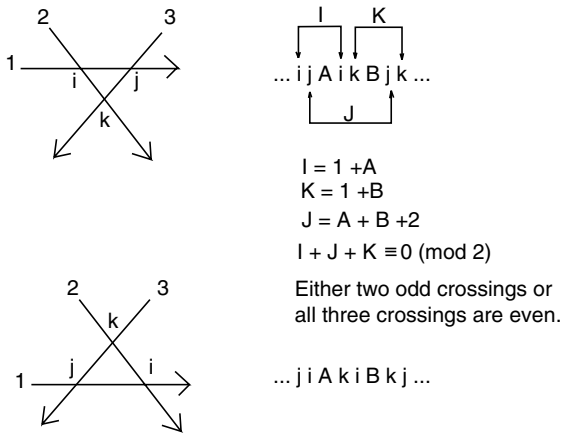


Fig. 14. Gaussian parities at the third Reidemeister move.

Furthermore it follows from the figure that the crossings labeled  $i, j, k$  in the before and after figures for the Reidemeister move have the same parity. It is then easy to see, using this information, that  $J(K)$  is invariant under virtual isotopy. We will refer to this figure again in the next subsection where we discuss the parity bracket.

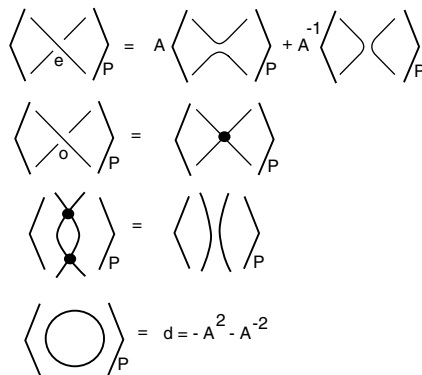
### 3.2. The parity bracket

In this section we introduce the Manturov Parity Bracket [23, 24]. This is a form of the bracket polynomial defined for virtual knots and for free knots that uses the parity of the crossings. To compute the parity bracket, we first make all the odd crossings into graphical vertices. Then we expand the resulting diagram on the remaining even crossings. The result is a sum of graphs with polynomial coefficients.

More precisely, let  $K$  be a virtual knot diagram. Let  $E(K)$  denote the result of making all the odd crossings in  $K$  into graphical nodes as illustrated in Fig. 15. Let  $SE(K)$  denote the set of all bracket states of  $E(K)$  obtained by smoothing each classical crossing in  $E(K)$  in one of the two possible ways. Then we define the *parity bracket*

$$\langle K \rangle_P = (1/d) \sum_{S \in SE(K)} A^{i(S)} [S],$$

where  $d = -A^2 - A^{-2}$ ,  $A^{i(S)}$  denotes the product of  $A$  or  $A^{-1}$  from each smoothing site according to the conventions of Fig. 15, and  $[S]$  denotes the reduced class of the virtual graph  $S$ . The graphs are subject to a reduction move that eliminates bigons as in the second Reidemeister move on a knot diagram as shown in Fig. 15. Thus  $[S]$  represents the unique minimal representative for the virtual graph  $S$  under virtual graph isotopy coupled with the bigon reduction move. A graph that reduces to a circle (the circle is a graph for our purposes) is replaced by the value  $d$  above.



$A = 1$  and  $d = -2$  for free knots.  
(Modulo 2 for Free Knots, the loop value is 0.)

Fig. 15. Parity bracket expansion.

Thus  $\langle K \rangle_P$  is an element of a module generated by reduced graphs with coefficients Laurent polynomials in  $A$ .

With the usual bracket polynomial variable  $A$ , the parity bracket is an invariant of standard virtual knots. With  $A = \pm 1$  it is an invariant of flat virtual knots. Even more simply, with  $A = 1$  and taken modulo two, we have an invariant of flat knots with loop value zero. See Fig. 16 for an illustration of the application of the parity bracket to the Kishino diagram illustrated there. The Kishino diagram is notorious for being hard to detect by the usual polynomial invariants such as the Jones polynomial. It is a perfect example of the power of the parity bracket. All the crossings of the Kishino diagram are odd. Thus there is exactly one term in the evaluation of the Kishino diagram by the parity bracket, and this term is the Kishino diagram itself, with its crossings made into graphical nodes. The resulting graph is irreducible and so the Kishino diagram becomes its own invariant. We conclude that this diagram will be found from any isotopic version of the Kishino diagram. This allows strong conclusions about many properties of the diagram. For example, it is easy to check that the least surface on which this diagram can be represented with the given planar cyclic orders at the nodes is genus two. Thus we conclude that the least genus for a surface representation of the Kishino diagram as a flat knot or virtual knot is two.

Two virtual knots or links that are related by a  $Z$ -move have the same standard bracket polynomial. This is proved in [9, 10] as a direct consequence of the bracket expansion formula. We would like to analyze the structure of  $Z$ -moves using the parity bracket. In order to do this we need a version of the parity bracket that is invariant under the  $Z$ -move. In order to accomplish this, we need to add a corresponding  $Z$ -move in the graphical reduction process for the parity bracket. This extra graphical reduction is indicated in Fig. 11 where we show a graphical  $Z$ -move along with flat and standard  $Z$ -moves and elementary consequences of these moves. The reader will note that graphs that are irreducible without the graphical  $Z$ -move can become reducible if we allow graphical  $Z$ -moves in the reduction process. For example, the graph associated with the Kishino knot is reducible under graphical  $Z$ -moves. However, there are examples of graphs that are not reducible

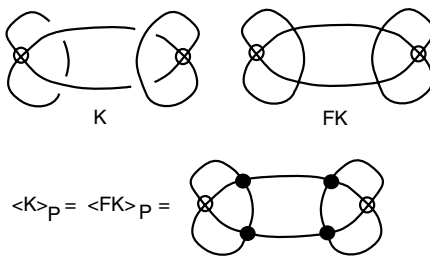


Fig. 16. Parity bracket detects the Kishino diagram.

under graphical  $Z$ -moves and Reidemeister two moves. To obtain invariants of free knots using the parity bracket, we adopt the graphical  $Z$ -move, since we need this invariance for free knots.

### 3.3. The parity bracket for free knots

This section explains the theory of the parity bracket for free knots. This section is written more formally than the previous section and provides a systematic example of the use of parity in handling a state sum invariant of free knots. Much of this material appears in [22, 23] and some of it in [17]. We include it here, both for the sake of completeness and because the newer invariants discussed in this paper can be used to go beyond what this approach can accomplish. See Sec. 5 for this discussion. Some terminology will be useful: We refer to the *graph* of a free knot as the intersection graph of its Gauss diagram. That is, the nodes of the graph are in one-to-one correspondence with the chords of the Gauss diagram, and two nodes are joined by an edge when the two chords intersect in the Gauss diagram. If a graph  $\Gamma$  is the intersection graph for the Gauss diagram of a free knot, we say that the free knot is *generated* by  $\Gamma$ . The reader should note that intersection graphs have neither loops nor bigons. In Fig. 17 we illustrate the relationship of an intersection graph and its Gauss diagram.

**Definition 5.** We call a free knot diagram *odd* if all of the nodes in its intersection graph have odd degree. (This is the same as saying that every crossing has odd Gaussian parity). We call a simple (no more than one edge between any two nodes) graph *irreducibly odd* if it is odd and for every pair of nodes  $u$  and  $v$  there is a third node  $w$  that is adjacent to exactly one of  $u$  and  $v$ .

The simplest example of an irreducibly odd graph is depicted in Fig. 17. Assume an irreducibly odd graph  $G$  generates a free knot  $K$ . It turns out that the representative  $G$  of the knot  $K$  is indeed *minimal*: any other representative of  $K$  has at least as many vertices as  $G$ . To this end, we shall describe a powerful invariant [23, 24] that captures graphical information about the free knot; but first we should introduce some notation.

Let  $\mathfrak{G}$  be the set of all equivalence classes of framed graphs with one unicursal component modulo second Reidemeister moves. Note that we do not ask for any

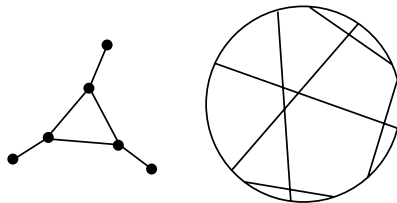


Fig. 17. An irreducibly odd graph and its chord diagram.

other types of Reidemeister moves for these graphs. When speaking of Reidemeister moves on such graphs, we shall usually indicate the move by saying an “R-2” move. We hope that the differences will be otherwise clear from the context. (Recall that framed locally four-valent graphs generalize the concept of a link diagram where every edge has an edge paired with it by skipping one edge in the cyclic order of edges at the node. We can then trace a path on a framed graph just as one traces a link component on a link diagram. A graph is *unicursal* when it can be completely traced by one such path that crosses each node twice.) Consider the linear space  $\mathbb{Z}_2\mathfrak{G}$ . Let  $G$  be a framed graph, let  $v$  be a vertex of  $G$  with four incident half-edges  $a, b, c, d$ , such that  $a$  is opposite to  $c$  and  $b$  is opposite to  $d$  at  $v$ . By *smoothing* of  $G$  at  $v$  we mean any of the two framed 4-regular graphs obtained by removing  $v$  and repasting the edges as  $a - b, c - d$  or as  $a - d, b - c$ , see Fig. 18.

Herewith, the rest of the graph (together with all framings at vertices except  $v$ ) remains unchanged. We may then consider further smoothings of  $G$  at *several* vertices. Consider the following sum

$$[G] = \sum_{s \text{ even, 1 comp}} G_s, \tag{3.1}$$

which is taken over all smoothings in all *even* vertices, and only those summands are taken into account where  $G_s$  has one unicursal component. This is the mod-2 parity bracket, where the loop value for more than one loop in state is zero. *Note that we do not make non-virtual odd nodes in the diagram into specially indicated graphical vertices. We just do not smooth them, but they are still subject to the Z-move and to reduction in the form of a second R-2 move. Thus in this state summation the remaining nodes take the role of the graphical vertices we previously described for the parity bracket.*

Thus, if  $G$  has  $k$  even vertices, then  $[G]$  will contain at most  $2^k$  summands, and if all vertices of  $G$  are odd, then we shall have exactly one summand, the graph  $G$  itself. Consider  $[G]$  as an element of  $\mathbb{Z}_2\mathfrak{G}$ . In this case it is evident that if all vertices of  $G$  are odd then  $[G] = G$  (here  $G$  is taken as a single graph to be reduced by R-2 moves).

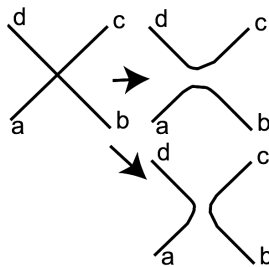


Fig. 18. Two smoothings of a vertex of for a framed graph.

**Theorem 1.** *If  $G$  and  $G'$  represent the same free knot then in  $\mathbb{Z}_2\mathfrak{G}$  the following equality holds:  $[G] = [G']$ .*

Theorem 1 yields the following.

**Corollary 1.** *Let  $G$  be an irreducibly odd framed 4-graph with one unicursal component. Then any representative  $G'$  of the free knot  $K_G$ , generated by  $G$ , has a smoothing  $\tilde{G}$  having the same number of vertices as  $G$ . In particular,  $G$  is a minimal representative of the free knot  $K_G$  with respect to the number of vertices.*

It turns out that elements from  $\mathbb{Z}_2\mathfrak{G}$  are easily encoded by their minimal representatives. More precisely, the following lemma holds.

**Lemma 1.** *Every four-valent framed graph  $G$  with one unicursal component considered as an element of  $\mathbb{Z}_2\mathfrak{G}$  has a unique irreducible representative, which can be obtained from  $G$  by consecutive application of second decreasing R-2 moves.*

This allows one to recognize elements  $\mathbb{Z}_2\mathfrak{G}$  easily, which makes the invariants constructed in the previous subsection digestable. In particular, the minimality of a framed 4-regular graph in  $\mathbb{Z}_2\mathfrak{G}$  is easily detectable: one should just check all pairs of vertices and see whether any of them can be cancelled by a second R-2 move (or in  $\mathbb{Z}_2\mathfrak{G}$  one should also look for free loops). Create all minimal representatives in this way, and then compare them. Indeed, we see that two graphs are R-2-equivalent if their minimal representatives coincide.

**Proof of Corollary 1.** By definition of  $[G]$  we have  $[G] = G$ . Thus if  $G'$  generates the same free knot as  $G$  we have  $[G'] = G$  in  $\mathbb{Z}_2\mathfrak{G}$ . Consequently, the sum representing  $[G']$  in  $\mathfrak{G}$  contains at least one summand which is  $a$ -equivalent ( $a$ -equivalent means equivalent by R-2 moves only) to  $G$ . Thus  $G'$  has at least as many vertices as  $G$  does. Moreover, the corresponding smoothing of  $G'$  is a diagram, which is  $a$ -equivalent to  $G$ . One can show that under some (quite natural) “rigidity” condition this will yield that one of smoothings of  $G'$  coincides with  $G$ .  $\square$

The use of parity gives this bracket considerable power. For example, consider the diagram in Fig. 12. We see that all the crossings in this free knot are odd. Thus the parity bracket is just the diagram itself seen as a graph and reduced by 2-moves. The reader can check that this graph is in fact irreducible in the free sense (see definition above) and the invariant of this free knot is the diagram itself as an irreducible graph. This not only means that this free knot is non-trivial, it also means that any diagram of this free knot will have states that reduce to the diagram in Fig. 12.

Parity is clearly an important theme in virtual knot theory and will figure in many future investigations of this subject. The type of construction that we have indicated for the bracket polynomial in this section can be varied and applied to other invariants. Furthermore the notion of describing a parity for crossings in a

diagram is also susceptible to generalization. For more on this theme the reader should consult [5, 12, 23, 24, 26, 27] for a use of parity for another variant of the bracket polynomial.

#### 4. Construction of the Main Invariants

In this section we shall describe the details of the construction of the  $\mathfrak{sl}(3)$  and  $G_2$  invariants. The  $C_2$  invariant has been treated in [28] and we will not repeat the construction details here. In all cases of these invariants, the work of verification involves checking consistency of the graphical expansions in situations where two polygons that are subject to expansion share an edge or edges. We shall call such a sharing of edges by polygons a *concurrency*. In our combinatorial approach, such concurrences must be calculated in detail. In some cases we show these detailed calculations in the paper. In other cases we give the reader instructions for doing the calculation. The purpose of this section is to organize these matters for the reader. It is clear to us that a less calculational approach to the theory of these invariants would be preferable, and we will explore that theory in a separate paper.

##### 4.1. The Kuperberg $\mathfrak{sl}(3)$ bracket

View Fig. 1. This figure gives the reduction relations for the Kuperberg  $\mathfrak{sl}(3)$  bracket. The invariant is originally defined for oriented classical links expressed as planar link diagrams. The expansion formulas at the top of the figure can be regarded as indicating an expansion of the link diagram into a state sum of specially oriented graphs with trivalent vertices. Note that each trivalent vertex has either three edges oriented into the vertex (a sink) or three edges oriented away from the vertex. The further relations in this figure can be used to eliminate all the graphs for planar link diagrams, resulting in a Laurent polynomial evaluation for the Kuperberg bracket. We shall generalize this invariant to virtual diagrams and find that there can be irreducible graphs in the expansion for virtual link. We begin by formalizing these graphical notions.

Let  $\mathcal{S}$  be the collection of all trivalent bipartite graphs with edges oriented from vertices of the first part to vertices of the second part of the bipartite division of the graph. Let  $\mathcal{T} = \{t_1, t_2, \dots\}$  be the (infinite) subset of connected graphs from  $\mathcal{S}$  having neither bigons nor quadrilaterals. Let  $\mathcal{M}$  be the module  $\mathbb{Z}[A, A^{-1}][t_1, t_2, \dots]$  of formal commutative products of graphs from  $\mathcal{T}$  with coefficients that are Laurent polynomials in one variable  $A$ . Disjoint unions of graphs are treated as products in  $\mathcal{M}$ . Our main invariant will be valued in  $\mathcal{M}$ .

**Statement 1.** Figure 1 shows the reduction moves for the Kuperberg  $\mathfrak{sl}(3)$  bracket. The last three lines of the figure will be called the *relations* in that figure. There exists a unique map  $f : \mathcal{S} \rightarrow \mathcal{M}$  which satisfies the relations in Fig. 1. The resulting evaluation yields a topological invariant of virtual links when the first two lines of

Fig. 1 are used to expand the link into a sum of elements of  $\mathcal{S}$ . We shall often identify the image of a graph with its image under the map  $f : \mathcal{S} \rightarrow \mathcal{M}$  in the module  $\mathcal{M}$ .

**Proof.** The relations we are going to use to prove the statement are as shown in Fig. 1. Note that for the case of planar tangles this map to diagrams modulo relations was constructed explicitly by Kuperberg [19], and the image was in  $\mathbb{Z}[A, A^{-1}]$ . We are going to follow [19], however, in the non-planar case, the graphs cannot be reduced just to collections of closed curves (in the case of the plane, Jordan curves) and so later evaluate to polynomials. In fact, irreducible graphs will appear in the non-planar case. First, we treat every 1-complex with all components being graphs from  $\mathcal{S}$  and circles: We treat that 1-complex as the formal product of these graphs, where each circle evaluates to the factor  $(A^6 + A^{-6} + 1)$ . We note that if a graph  $\Gamma$  from  $\mathcal{S}$  has a bigon or a quadrilateral, then we can use the relations shown in Fig. 1 (resolution of quadrilaterals, resolution of bigons, loop evaluation) to reduce it to a smaller graph (or two graphs, then we consider it as a product). So, we can proceed with resolving bigons and quadrilaterals until we are left with a collection of graphs  $t_j$  and circles; this gives us an element from  $\mathcal{M}$ ; once we prove the uniqueness of the resolution, we set the stage for proving the existence of the invariant. We must carefully check well-definedness and topological invariance.

In what follows, we shall often omit the letter  $f$  by identifying graphs with their images or intermediate graphs which appear after some concrete resolutions.

Our goal is to show that this map  $f : \mathcal{S} \rightarrow \mathcal{M}$  is well-defined. We shall prove it by induction on the number of graph edges. *The induction base is obvious* and we leave its articulation to the reader. To perform the induction step, notice that all of Kuperberg's relations are *reductive*: from a graph we get to a collection of simpler graphs.

Assume for all graphs with at most  $2n$  vertices that the statement holds. Now, let us take a graph  $\Gamma$  from  $\mathcal{S}$  with  $2n + 2$  vertices. Without loss of generality, we assume this graph is connected. If it has neither bigon nor quadrilateral, we just take the graph itself to be its image. Otherwise we use the relations *resolution of bigons* or *resolution of quadrilaterals* as in Fig. 1 to reduce it to a linear combination of simpler graphs; we proceed until we have a sum (with Laurent polynomial coefficients) of (products of) graphs without bigons and quadrilaterals.

According to the induction hypothesis, for all simpler graphs, there is a unique map to  $\mathcal{M}$ . However, we can apply the relations in different ways by starting from a given quadrilateral or a bigon. We will show that the final result does not depend on the bigon or quadrilateral we start with. To this end, it suffices to prove that if  $\Gamma$  can be resolved to  $\alpha\Gamma_1 + \beta\Gamma_2$  from one bigon (quadrilateral) and also to  $\alpha'\Gamma'_1 + \beta'\Gamma'_2$  from the other one, then both linear combinations can be resolved further, and will lead to the same element of  $\mathcal{M}$ . This will show that final reductions are unique.

Whenever two nodes of a quadrilateral coincide, then two edges coincide and it is no longer subject to the quadrilateral reduction relation. Thus we assume



that quadrilaterals under discussion have distinct nodes. Note that if two polygons (bigons or quadrilaterals) share no common vertex then the corresponding two resolutions can be performed *independently* and, hence, the result of applying them in any order is the same. So, in this case,  $\alpha\Gamma_1 + \beta\Gamma_2$  and  $\alpha'\Gamma'_1 + \beta'\Gamma'_2$  can be resolved to the same linear combination in one step. By the hypothesis,  $f(\Gamma_1), f(\Gamma_2), f(\Gamma'_1), f(\Gamma'_2)$  are all well defined, so, we can simplify the common resolution for  $\alpha\Gamma_1 + \beta\Gamma_2$  and  $\alpha'\Gamma'_1 + \beta'\Gamma'_2$  to obtain the correct value for  $f$  of any of these two linear combinations, which means that they coincide.

If two polygons (bigons or quadrilaterals) share a vertex, then they share an edge because the graph is trivalent. If a connected trivalent graph has two different bigons sharing an edge then the total number of edges of this graph is three, and the evaluation of this graph in  $\mathcal{T}$  follows from an easy calculation. Therefore, let us assume we have a graph  $\Gamma$  with an edge shared by a bigon and a quadrilateral. We can resolve the quadrilateral first, or we can resolve the bigon first. The calculation in Fig. 19 shows that after a two-step resolution we get to the same linear combination.

A similar situation happens when we deal with two quadrilaterals sharing an edge, see Fig. 20. Here we have shown just one particular resolution, but the picture is symmetric, so the result of the resolution when we start with the right quadrilateral, will lead us to the same result. See also Figs. 21–23. These figures illustrate two other ways in which the edge can be shared. Note that Figs. 21 and 22 illustrate

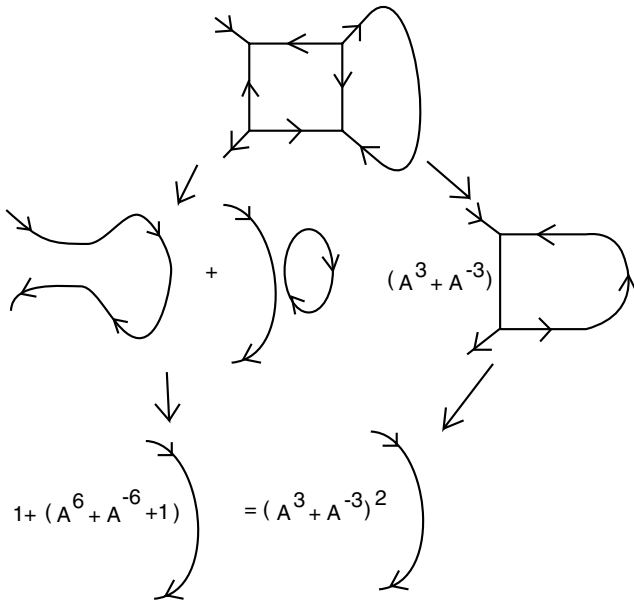


Fig. 19. Two ways of reducing a quadrilateral and a bigon.

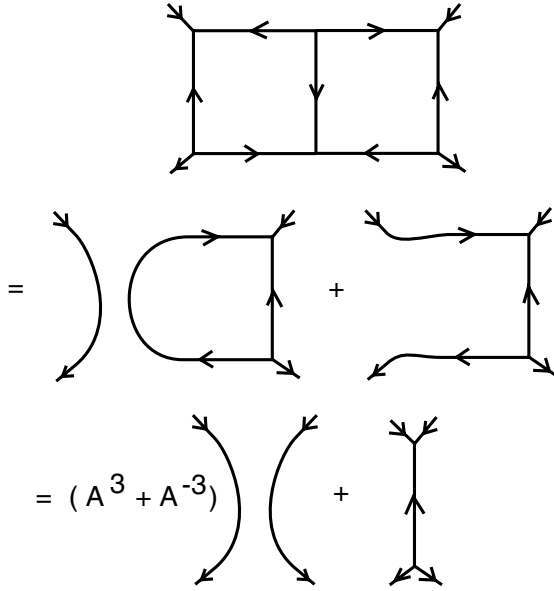


Fig. 20. Resolving two adjacent squares.

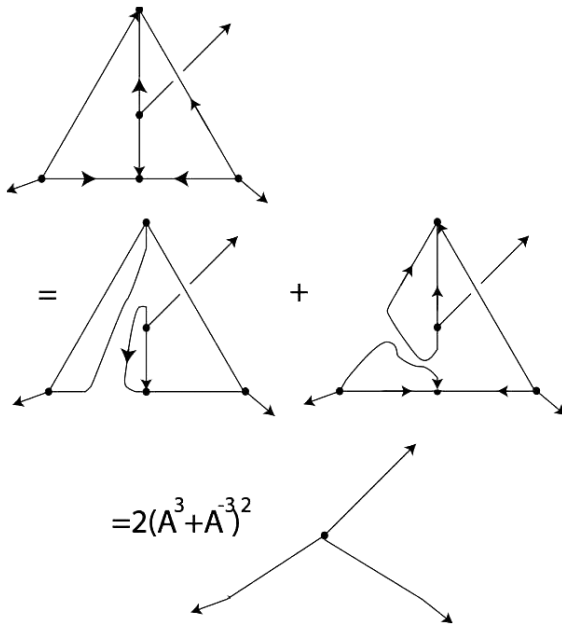


Fig. 21. Resolving two different adjacent squares.

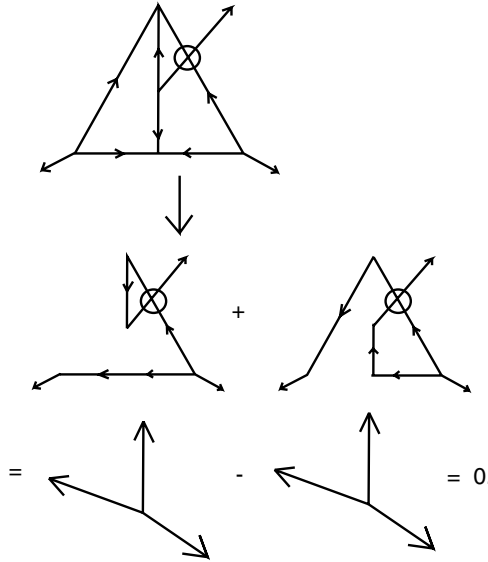


Fig. 22. Resolving two different adjacent squares with virtual crossing.

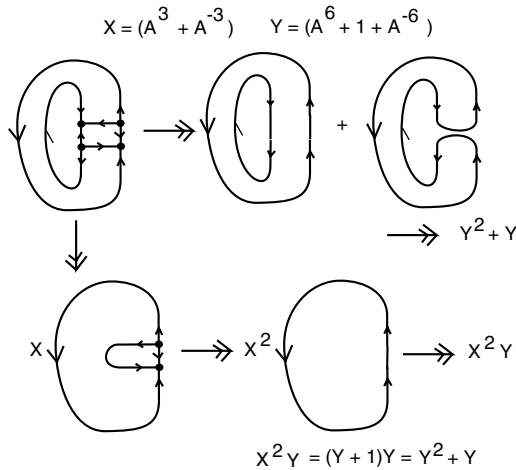


Fig. 23. Resolving two annular squares.

a possibly non-planar case and a virtual case, and that we use the abstract graph structure (with a signed choice of relative order at the trivalent vertex as in Fig. 1) in the course of the evaluation. These cases cover all the ways that shared edges can occur, as the reader can easily verify.

Thus, we have performed the induction step and proved the well-definiteness of the mapping. Note that the ideas of the proof are the same as in the classical case;

however, we never assumed any planarity of the graph; we just drew graphs planar whenever possible. Note that the situation in Fig. 21 is principally non-planar. The invariance under the  $Z$ -move follows from this definition because the graphical pieces into which we expand a crossing, as in Fig. 1, are, as graphs, symmetric under the interchange produced by the  $Z$ -move.  $\square$

**Remark.** We can, in the case of flat knots or standard virtual knots represented on surfaces, enhance the invariant by keeping track of the embedding of the graph in the surface and only expanding on bigons and quadrilaterals that bound in the surface. We will not pursue this version of the invariant here. In undertaking this program we will produce evaluations that are not invariant under the  $Z$ -move for flats or for virtual knots.

Now we give a formal description of our main invariant. This evaluation is invariant under the  $Z$ -move. It is defined for virtual knots and links and it specializes to an invariant of free knots. Let  $K$  be an oriented virtual link diagram. With every classical crossing of  $K$ , we associate two local states: the *oriented* one and the *unoriented* one: the oriented one shown as an oriented smoothing in Fig. 1, and the unoriented one shown as a connection of two trivalent nodes in Fig. 1. A *state* of the diagram is a choice of local state for each crossing in the diagram.

We define the bracket  $[[\cdot]]$  (generalized Kuperberg  $sl(3)$  bracket) as follows. Let  $K$  be an oriented virtual link diagram. For a state  $s$  of a virtual knot diagram  $K$ , we define the weight of the state as the coefficient of the corresponding graph according to the Kuperberg relations (Fig. 1). More precisely, the weight of a state is the product of weights of all crossings, where a weight of a positive crossing is  $A^{2wr}$  for the oriented resolution and  $-A^{-wr}$  for the unoriented resolution,  $wr$  stands for the writhe number (the oriented sign) of the crossing.

Set

$$[[K]] = \sum_s w(K_s) \cdot f(K_s) \in \mathcal{M}, \tag{4.1}$$

where  $w(s)$  is the weight of the state.

**Theorem 2.** *For a given virtual diagram  $K$ , the normalized bracket  $(A^{-8wr(K)})[[K]]$  is invariant under all Reidemeister moves and the  $Z$ -move. Recall that  $wr(K)$  denotes the writhe obtained by summing the signs of all the classical crossings in the corresponding diagram.*

**Proof.** The invariance proof under Reidemeister moves repeats that of Kuperberg. Note that the writhe behavior is a consequence of the relations in Fig. 1. The only thing we require is that the Kuperberg relations (summarized in Fig. 1) can be applied to yield unique reduced graph polynomials. The discussion preceding the proof, proving Statement 1, handles this issue.  $\square$

From the definition of  $[[K]]$  we have the following.

**Corollary 2.** *If  $[[K]]$  does not belong to  $\mathbb{Z}[[A, A^{-1}]] \subset \mathcal{M}$  then the knot  $[[K]]$  is not classical. That is, if non-trivial graphs appear in the evaluation, then the knot is not classical.*

Recalling that a free link is an equivalence of virtual knots modulo  $Z$ -moves and crossing switches and taking into account that the skein relations of Fig. 1 for  $[[\cdot]]$  for  $\times$  and  $\times$  are the same when specifying  $A = 1$ , we get the following.

**Corollary 3.**  *$[[K]]_{A=1}$  and  $[[K]]_{A=-1}$  are invariants of free links.*

By the unoriented state  $K_{\text{us}}$  of virtual knot diagram (respectively, free knot diagram)  $K$  we mean the state of  $K$  where all crossings are resolved in the unoriented fashion where the crossing is replaced by two connected trivalent nodes.

**Notation.**  $K_{\text{us}}$ . Note that  $K_{\text{us}}$  is treated as a graph.

**Corollary 4.** *Assume for a virtual knot (or free knot)  $K$  with  $n$  classical crossings the graph  $K_{\text{us}}$  has neither bigons nor quadrilaterals. Then every knot  $K'$  equivalent to  $K$  has a state  $s$  such that  $K'_s$  contains  $K_{\text{us}}$  as a subgraph. This state can be treated as an element of  $\mathcal{M}$ . In particular,  $K$  is minimal.*

Note that the coincidence of  $K_{\text{us}}$  and  $K'_{\text{us}}$  does not guarantee the coincidence of  $K$  and  $K'$ . For example, if  $K$  and  $K'$  differ by a third unoriented Reidemeister move, then, of course,  $[[K]] = [[K']]$ . The corresponding resolutions  $K_{\text{us}}$  and  $K'_{\text{us}}$  will coincide (they will have a hexagon inside).

**Corollary 5.** *Let  $K$  be a four-valent framed graph with  $n$  crossings and girth number at least five. Then the hypothesis of Corollary 4 holds.*

So, this proves the minimality of a large class of framed four-valent graphs regarded as free knots: all graphs having girth  $\geq 5$  and many other knots. For example, consider the free knot  $K_n$  whose Gauss diagram is the  $n$ -gon,  $n > 6$ : it consists of  $n$  chords where  $i$ th chord is linked with exactly two chords, those having numbers  $i - 1$  and  $i + 1$  (the numbers are taken modulo  $n$ ). Then  $K_n$  satisfies the condition of Corollary 4 and, hence, is minimal in a strong sense.

Note that the triviality of such  $n$ -gons as free knots was proven only for  $n \leq 6$ .

**Remark 1.** The above argument works for links and tangles as well as knots.

From the construction of  $[[\cdot]]$  we get the following corollary.

**Corollary 6.** *Let  $K$  be a virtual (respectively, flat) knot, and let  $\Gamma_1 \cdots \Gamma_k$  be a product of irreducible graphs which appear as a summand in  $[[K]]$  (respectively,  $[[K]]_{A=1}$ ) with a non-zero coefficient. Then the minimal virtual crossing number of  $K$  is greater than or equal to the sum of crossing numbers of graphs:  $cr(\Gamma_1) + \cdots + cr(\Gamma_k)$  and the underlying genus of  $K$  is less than or equal to the sum of genera  $g(\Gamma_1) + \cdots + g(\Gamma_k)$  (in virtual or free knot category).*

The above corollary easily allows one to reprove the theorem first proved in [26], that the number of virtual crossings of a virtual knot grows quadratically with respect to the number of classical crossings for some families of graphs. In [26], it was done by using the parity bracket. Now, we can do the same by using

$$\text{Free}[[K]] = [[K]]|_{A=1}.$$

With this invariant one can easily construct infinite series of trivalent bipartite graphs which serve as  $K_{us}$  for some sequence of knots  $K_n$  and such that the minimal crossing number for these graphs grows quadratically with respect to the number of crossings. Recalling that the number of vertices comes from the number of classical crossings of  $K_n$ , we get the desired result.

#### 4.2. The generalized Kuperberg $G_2$ bracket

The analysis for the Kuperberg  $G_2$  invariant follows the same lines as our analysis for the  $\text{sl}(3)$  invariant. The expansion rules for this invariant are given in Figs. 3–5. It is implicit in Kuperberg’s work that concurrences of bigons, triangles, quadrilaterals and pentagons that do not involve virtual crossings lead to consistent results for the  $q$  variable indicated in these figures. We do not repeat these verifications here. However, when we make the analysis with concurrences involving virtual crossings we find that it is in fact necessary to restrict to the case of flat virtual knots or free knots in order to obtain consistency. Thus we take  $q = 1$  for our  $G_2$  invariant. The reasons for restricting to  $q = 1$  becomes apparent from the verifications but we will not show the details here.

Along with restricting to  $q = 1$  we have to explain how to handle the reduction calculus for virtual graph diagrams in the plane. A graph diagram in the plane may have (flat) 4-regular crossings and trivalent crossings. Each such crossing is endowed with a cyclic order by its embedding in the plane. For flat virtual knots we do not allow the cyclic order at a crossing to change. This means that for flat knots, we do not consider the reduction of concurrences of polygons that involve virtual crossings that cannot be isotoped away from the polygon. For example, view Fig. 31 where we have a four-sided region that can be reduced and a five-sided region that has a virtual intersecting arc. We can for free knots perform the reduction of the four-sided region, but there is no way to reduce the five-sided region. Consequently there is no need for the free-knot  $G_2$  invariant to examine, as is shown in the figure, what will happen when we change a local cyclic order and reduce the five-sided region. For the invariant of free knots that we are about to describe, we need that the results of expansion from the two local drawings in Fig. 31 give the same results. We will discuss that below.

The reader should now see that the  $G_2$  invariant has two distinct flavors, one for flat virtual knots and links and one for free knots and links. The free knot version involves more checking for concurrences than the flat knot version. One can verify that for those that do not involve virtual crossings such as illustrated in Figs. 27–29

the expansions are independent of which polygon is first expanded. This provide the proof of validity for the flat knot invariant. The flat knot invariant is of interest, but it should be pointed out that flat virtual knots and links are fully classified via [4, 6].

**The  $G_2$  invariant for free knots.** For free knots, we allow the  $Z$ -move as part of the equivalence relation, and hence allow the corresponding change in cyclic order at a trivalent vertex. For the trivalent vertices we use the rule indicated in Fig. 4 that shows a change of sign if there is a transposition applied to the cyclic order at a trivalent vertex. That is, the invariant will be valued in an algebra of graphs with integer coefficients where there is an equivalence relation on the graphs generated by the reduction and transformation rules indicated in the figures such as the above and the ones we now discuss. We can formalize this just as we have already done for  $sl(3)$ . Furthermore, *we only allow reductions on bigons, triangles, quadrilaterals and pentagons that have an interior that is clear of any other aspects of the graph.* This principle is illustrated in Fig. 24 where we start with a quadrilateral that has an arc crossing it virtually. We change a cyclic order at one of its trivalent vertices, move the arc by a detour move, and then expand the quadrilateral.

**Definition 6.** We let  $\{\{K\}\}_{\text{Free}}$  and  $\{\{K\}\}_{\text{Flat}}$  denote the  $G_2$  invariants for  $K$  free and flat respectively.

**Definition 7.** By a *leading state* of a framed 4-regular graph  $G$  on  $n$  vertices (considered as a representative of a free link or a flat link) we mean a state where each of the  $n$  vertices is resolved with an additional edge.

Thus, every 4-regular graph  $G$  has  $4^n$  states in the expansion of  $\{\{G\}\}_{\text{Free}}$  or  $\{\{G\}\}_{\text{Flat}}$ ,  $2^n$  of which are leading. Note that all these graphs  $G_s$  corresponding

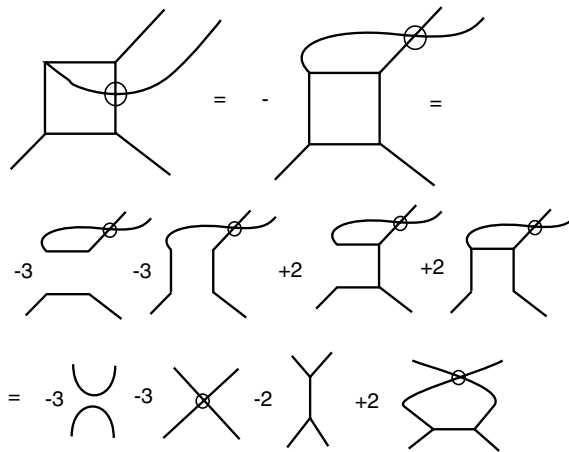


Fig. 24. Evaluating a virtual quad.

$$\begin{aligned}
 & \times = (1/2) \left[ \begin{array}{c} \text{---} \\ \text{---} \end{array} + \begin{array}{c} \text{---} \\ \text{---} \end{array} + \begin{array}{c} \text{---} \\ \text{---} \end{array} + \begin{array}{c} \text{---} \\ \text{---} \end{array} \right] \\
 & \text{---} \otimes \text{---} = \text{---} \otimes \text{---} = - \text{---} \otimes \text{---} \\
 \text{Therefore} & \quad \text{---} \otimes \text{---} = \text{---} \otimes \text{---} \quad \text{and,} \\
 & \text{---} \otimes \text{---} = \\
 & (1/2) \left[ \begin{array}{c} \text{---} \otimes \text{---} \\ \text{---} \otimes \text{---} \\ \text{---} \otimes \text{---} \\ \text{---} \otimes \text{---} \end{array} \right] \\
 & = (1/2) \left[ \begin{array}{c} \text{---} \otimes \text{---} \\ \text{---} \otimes \text{---} \\ \text{---} \otimes \text{---} \\ \text{---} \otimes \text{---} \end{array} \right] \\
 & = \text{---} \otimes \text{---} .
 \end{aligned}$$

Fig. 25.  $G_2$  evaluation is invariant under the  $Z$ -move.

$$\begin{aligned}
 & \bigcirc \quad \bigcirc \quad \longrightarrow \quad (-2)(-2) = 4. \\
 & \bigcirc \otimes \bigcirc \quad \longrightarrow \\
 & (1/2) \left[ \begin{array}{c} \bigcirc \otimes \bigcirc \\ \bigcirc \otimes \bigcirc \\ \bigcirc \otimes \bigcirc \\ \bigcirc \otimes \bigcirc \end{array} \right] \\
 & = (1/2) \left[ \begin{array}{c} \bigcirc + \bigcirc - \bigcirc - \bigcirc \end{array} \right] \\
 & = (1/2) \left[ \begin{array}{c} (-2) + (-2) - (-6)(-2) - (-6)(-2) \end{array} \right] \\
 & = -14.
 \end{aligned}$$

Fig. 26.  $G_2$  evaluation of simplest free link.



to various leading states  $S$ , appear in the expansion of  $\{\{G\}\}_{\text{Free}}$  (respectively,  $\{\{G\}\}_{\text{Flat}}$ ) with the coefficient  $1/2^n$ .

In Fig. 25 we show that the resulting flat virtual evaluation is invariant under the  $Z$ -move. Hence our  $G_2$  evaluation is defined on free knots. Note that we use crucially the sign changes from the reordering of cyclic vertices in this derivation. In both Figs. 24 and 25, we are using the  $q = 1$  value for the expansions. We leave it to the reader to see that this invariant will not work except at  $q = 1$ . Figure 26 shows the expansion and evaluation of the  $G_2$  invariant for the simplest free link. Figures 27–29 illustrate the consistency of polygon concurrences where there are no

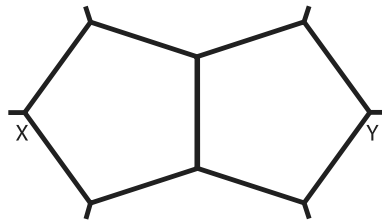


Fig. 27. Five and five direct.

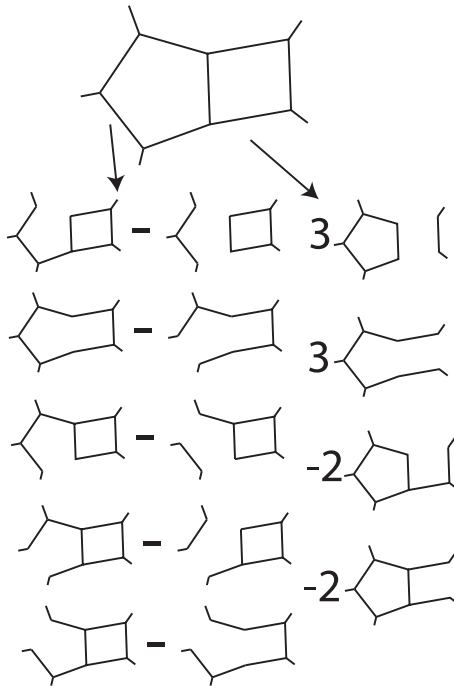


Fig. 28. Five and four direct.

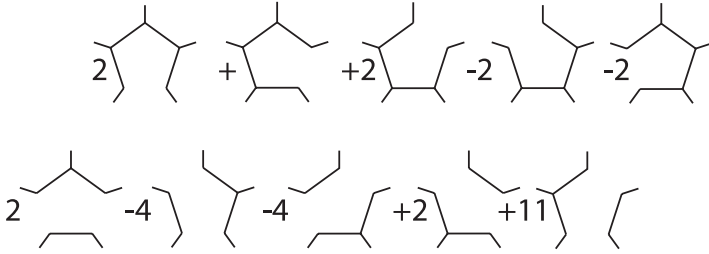


Fig. 29. End result of five and four.

local virtual crossings. Figures 30–34 illustrate aspects of concurrence consistency for four and five sided polygons. We have not given all details, but we have specified in this section how to make these expansions and compare them. For example, in Fig. 31 we point out that due to the change of cyclic order there should be a sign change when expanding on four versus five in this configuration. We assert that this does indeed happen and leave out the long details. In Fig. 32 we indicate a sign change due to cyclic order and that the right-hand side of the first equality can be transformed by a  $180^\circ$  rotation (keeping tangle ends fixed) to the left-hand side.

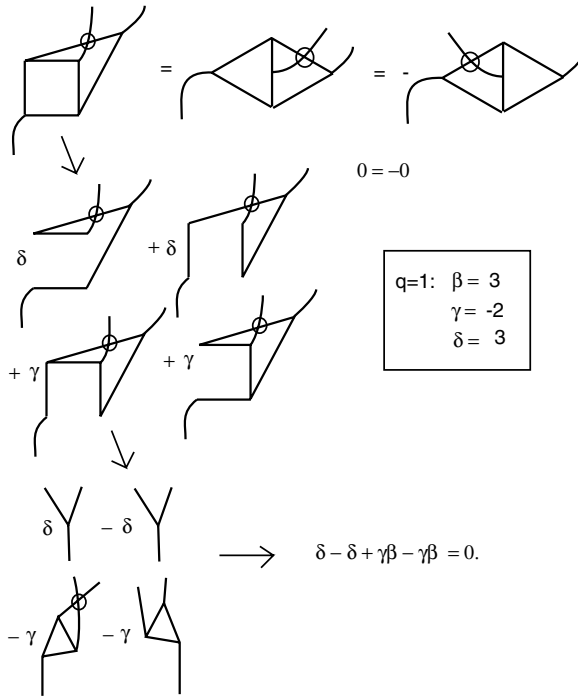


Fig. 30. Four interacting virtually with four.

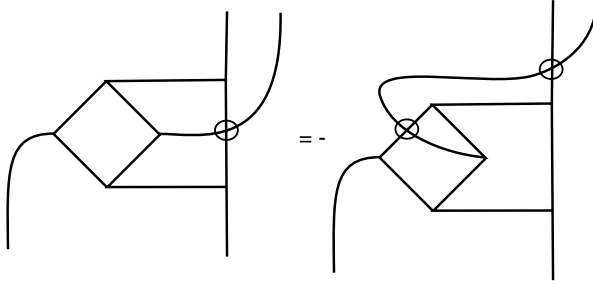


Fig. 31. Four interacting virtually with five.

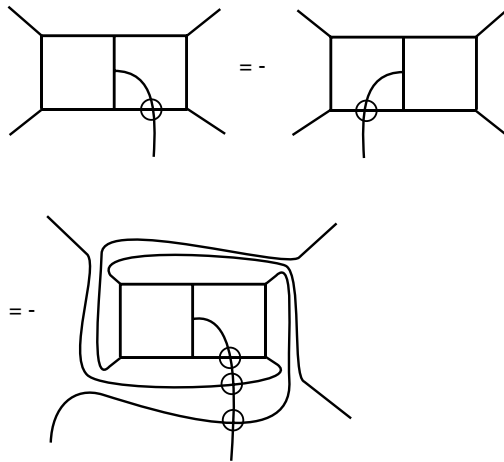


Fig. 32. Five interacting virtually with five twist identity.

This means that if we expand on just the left-hand side, the resulting expansion should go into the negative of itself under this tangle rotation. Figure 33 shows explicitly how certain free trivalent virtual tangles are transformed under the  $180^\circ$  rotation. The arrows on the tangle-boxes at the top of the figure are placed to remind the reader that the tangle-box turns through  $180^\circ$ , with the ends of the tangle (at its four corners) remaining fixed. Finally Fig. 34 shows the end-result of the expansion of the left-hand side of Fig. 32. It is then easy for the reader to check that this expansion does have the requisite property under the  $180^\circ$  rotation. This completes our sketch of the proof of the validity of the  $G_2$  invariant for free knots and links.

**Discussion.** For the  $sl(3)$  invariant, we have the advantage of using the orientation on the original free knot, which leads to the oriented states of the invariant and the restrictions to even numbers of sides to small polygons appearing in the expansion

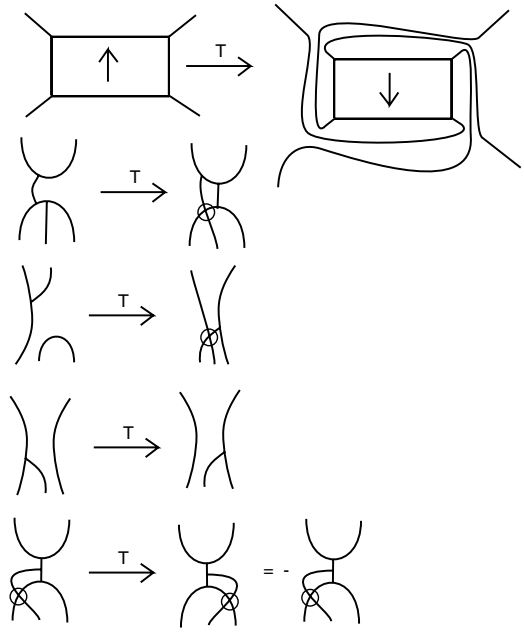


Fig. 33. Five interacting virtually with five insertions.

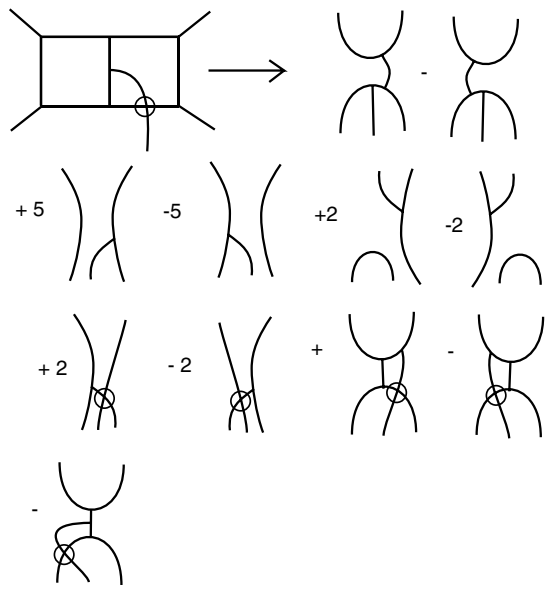


Fig. 34. Five interacting with five virtually — the expansion.

J. Knot Theory Ramifications 2015.24. Downloaded from www.worldscientific.com  
 by MATHEMATISCHES FORSCHUNGSINSTITUT OBERWOLFACH on 06/24/15. For personal use only.

of the knot to the states. The  $\mathfrak{sl}(3)$  invariant can be sometimes used to show non-invertibility of free knots. See [17].

We are now in possession of the  $G_2$  invariant for free knots and links. We shall refer to it as the *free  $G_2$  invariant* if necessary. If a diagram has no bigons, triangles, quadrilaterals or pentagons, then no reduction is possible and the resulting free knot is non-trivial via this invariant.

**Remark on the  $C_2$  invariant.** See Fig. 2 for the expansion and reduction rules for the  $C_2$  invariant. The main advantage of the  $C_2$  invariant is that if there are no triangles in the expansion to graphs of the free knot, then one can reconstruct the free knot from that expansion. Examine Fig. 2 and note that the  $\mathfrak{sl}(3)$  invariant can, if there are no triangles in the skein expansion, give us enough information to reconstruct a free knot. We refer to [28] for the theory of the  $C_2$  invariant. Its verification for free knots goes by the same lines as the verifications we have done here for  $\mathfrak{sl}(3)$  and  $G_2$ .

If there are triangles, then we can hope to use the  $G_2$  invariant to make a finer discrimination. We can combine the information already known from the  $\mathfrak{sl}(3)$  and  $C_2$  invariants to narrow down the possibilities for applying the  $G_2$  invariant. Thus we can assume that we have a diagram that has triangles in its skein expansion. Such an unoriented diagram slips through the discrimination of both the  $\mathfrak{sl}(3)$  and  $C_2$  invariants and can be tested with the  $G_2$  invariant. We will discuss the construction of such examples in Sec. 6.

## 5. Minimality Theorems and Uniqueness of Minimal Diagrams

The existence of non-trivial free knots was first proved in 2009 (see arXiv version of [22]. See also [23].). The proof relied upon the notion of *parity*: the way of discriminating between *even* and *odd* crossings of the knot diagram (respectively, chords of the Gauss diagram). The simplest example of parity is *the Gaussian parity* as described in Sec. 3. In Sec. 3, we have discussed Corollary 1 showing that an irreducible odd diagram of a free knot  $K$  is minimal in the strong sense that every diagram  $K'$  equivalent to  $K$  has a smoothing identical with  $K$ .

Corollary 1 of Sec. 3.3 is a strong statement. For example, it follows from it that the minimal diagram is unique: if  $K$  is an  $n$ -crossing diagram, then no other  $n$ -crossing diagram  $K'$  can have  $K$  as a smoothing since non-trivial smoothing leads to a smaller number of classical crossings. This result partially solves the recognition problem for free knots, but it is solved for a very small class of them. Indeed, there are lots of minimal diagrams of free knots which are minimal and have even crossings.

The result stated in Corollaries 4 and 5 does not claim the uniqueness of the minimal diagram. The main reason is that we cannot restore the initial knot (or

link)  $K$  from  $K_{\text{us}}$  in a unique way. Indeed, given a trivalent graph, in order to get a framed four-valent graph, we have to contract some edges (those corresponding to unoriented smoothings of vertices). This means that we have to find a matching for the set of vertices of the whole trivalent graph  $K_{\text{us}}$ . But there might be many matchings of this sort. After performing such a matching, we still do not have a free knot diagram (framed four-valent diagram), because we do not know which incoming edge is opposite to which emanating edge. Thus, there may be many diagrams  $K$  having the same  $K_{\text{us}}$ . Of course, in some cases, the whole invariant  $\{\{K\}\}_{\text{Free}}$  itself does distinguish between them, nevertheless, sometimes it is not the case. View Fig. 35. The bracket  $\{\{K\}\}_{\text{Flat}}$  is certainly invariant under any Reidemeister moves; so is  $K_{\text{us}}$  in the case of Corollary 4.

Now, we see that in Fig. 35, two diagrams which differ by a third Reidemeister move, lead to the same  $K_{\text{us}}$ . However, we do not know whether there are different minimal knot diagrams of different knot types sharing  $K_{\text{us}}$  (or, even, sharing  $\{\{K\}\}_{\text{Free}}$ ). If the unoriented third Reidemeister move were the only case when  $\{\{K\}\}_{\text{Free}}$  does not change then we would have not only a criterion for minimality of a large class of diagrams, but also a recognition algorithm for a large class of free knots.

A free knot diagram (a framed four-valent graph) cannot contain loops or bigons. If a free knot diagram  $K$  contains a triangle, then it is equivalent to a diagram  $K'$  obtained from  $K$  by a third Reidemeister move. If  $K$  has girth greater than or equal to four, then no decreasing Reidemeister move can be applied to  $K$  and no third Reidemeister move can be applied to  $K$ . Thus we arrive at the following natural conjecture about free knots.

**Conjecture 1.** *If a framed four-valent graph  $K$  has girth greater than or equal to 4 then this diagram is the unique minimal diagram for the knot class of  $K$ .*

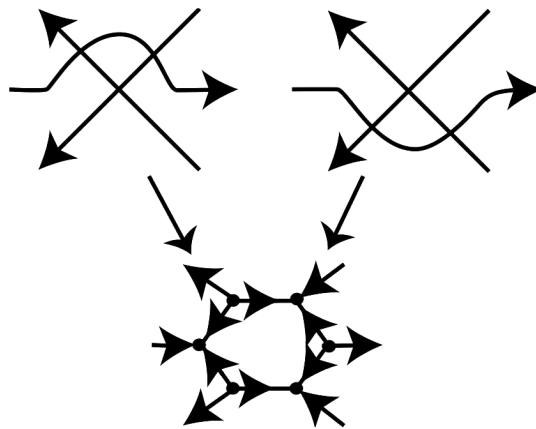


Fig. 35. The third move does not change the bracket.

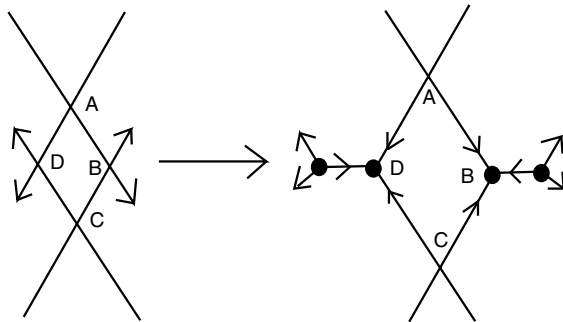


Fig. 36. Quadrilaterals of a special sort in  $K$  yield quadrilaterals in  $K_{us}$ .

In fact, the “minimality” part partially follows from Corollary 5. Indeed, all diagrams of girth 5 and many diagrams of girth 4 satisfy the conjecture. For a diagram of girth 4 to satisfy the conjecture, one should forbid the quadrilaterals of the following sort (see Fig. 36) which lead to quadrilaterals in  $K_{us}$ .

For such a quadrilateral, there are two opposite vertices (say,  $A$  and  $C$ ) such that all the four edges of the quadrilateral emanate from  $A$  and  $C$  (and come into the other two vertices,  $B$  and  $D$ ). Concerning the uniqueness of such minimal diagram, a very little is known because of the “matching ambiguity” discussed above.

### 5.1. Minimality related to $G_2$

**Definition 8.** Let  $G$  be a flat (respectively, free) trivalent graph. We shall say that  $G$  contains a graph  $G'$  if  $G'$  can be obtained from  $G$  by a sequence of the Kuperberg reduction rules for the flat (respectively, free)  $G_2$  invariant.

Let  $K$  be a flat (respectively, free) link diagram. Note that all those graphs  $K_s$  corresponding to various leading states  $s$  of  $K$ , appear in the expansion of  $\{\{K\}\}_{Free}$  (respectively,  $\{\{K\}\}_{Flat}$ ) with the coefficient  $1/2^n$ . Some of these graphs are reducible, and some of them are not. However, no irreducible leading states will cancel in the state sum. This leads to the following.

**Theorem 3.** Assume  $K$  be a flat (respectively, free) 4-regular graph, and let  $S$  be a leading state of  $K$  such that  $K_s$  is irreducible in the flat (respectively, free) category. Then every graph  $K'$  equivalent to  $K$  as a flat (respectively, free) link has a state that contains  $K_s$ .

In particular,  $G$  is minimal, non-classical and non-trivial.

Note that one can construct free knot diagrams satisfying the conditions of Theorem 3 with all even crossings, having some triangles and not satisfying minimality conditions for  $sl(3)$  and  $sl(3)$  graphical invariants for free knots. For example, this can be achieved by using Gauss diagrams.

### 6. Examples

This section gives examples related to the discussions in the paper. The first example we consider is given in Fig. 37. Here we have an example of a flat virtual link diagram  $L$ . In Fig. 38 we illustrate a state of this link in the expansion of the flat  $sl(3)$  bracket  $\{\{L\}\}_{Flat}$ . We call this the “octahedral state” of  $K$ . In Fig. 39 we show how the state (and hence the corresponding link) embeds in a surface with boundary. We now analyze this state graph  $G$  and show that it is irreducible in the  $sl(3)$  bracket expansion of  $K$ , thus proving that  $K$  is a non-trivial flat link.

Examine the surface  $S$  in Fig. 39 and it is apparent that it has four boundary components with the following numbers of edges from the graph for the corresponding faces: 8, 8, 16, 16. Thus there are no small faces in this graph and so it is not possible to make any reductions of the graph in the setting of the  $sl(3)$  invariant. It is not hard to see that this state receives a non-zero coefficient in the invariant, and hence the link  $L$  is a non-trivial flat link. Incidentally, if  $F$  is the surface obtained from  $S$  by adding a disk to each boundary component, and  $g$  is the genus of  $F$ , then we have  $v = 16, e = 24, f = 4$  where  $v, e, f$  denote the number of vertices, edges and faces of the corresponding decomposition of  $F$ . Then  $2 - 2g = v - e + f = 16 - 24 + 4 = -4$  and hence  $g = 3$ . The surface  $F$  has genus equal to three. Note that this means that the link  $L$  cannot be represented on any surface of genus smaller than 3 since the irreducible state graph  $G$  must appear in every such representation. Since  $L$  can be represented in genus three, this proves that  $L$  has surface genus three as a flat link.

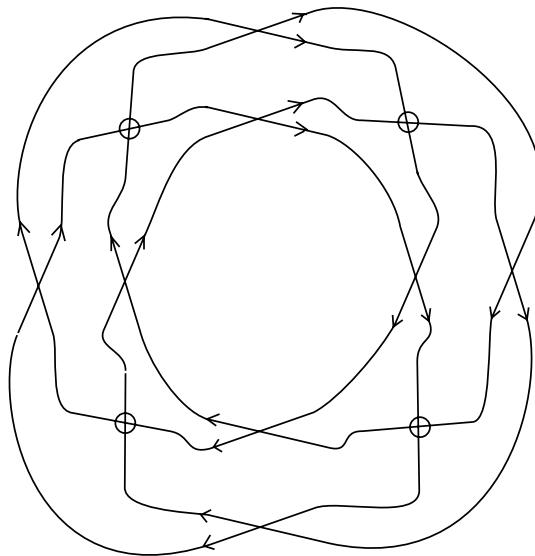


Fig. 37. The flat link  $L$ .



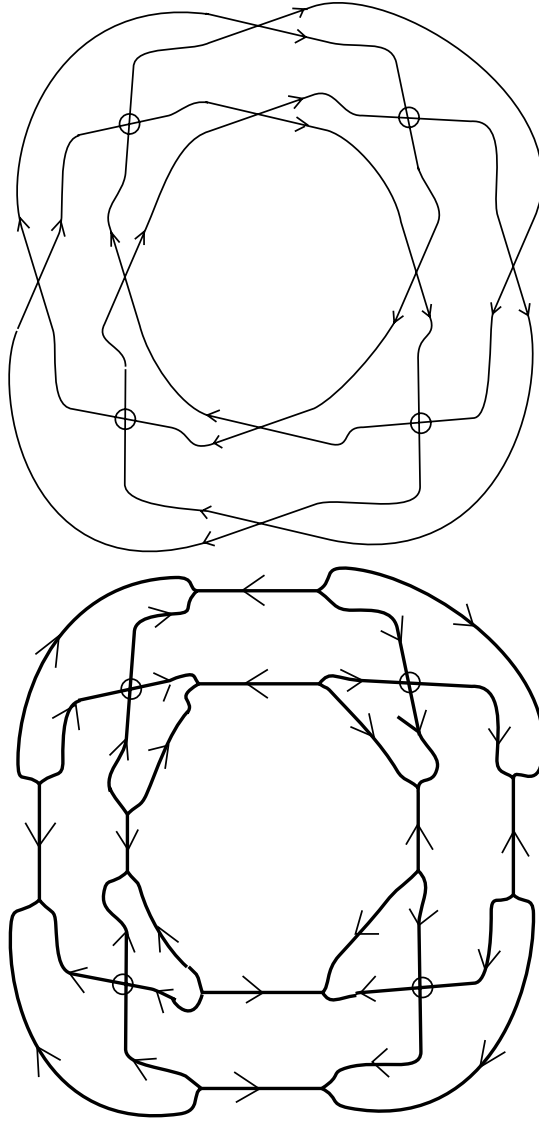


Fig. 38. A state of the flat link  $L$ .

The example shown in Fig. 40 may be a non-trivial free knot, but it is not detected by the invariants discussed in this paper.

The next example, depends on Figs. 41 and 42. In Fig. 42 we show a free knot  $G$  where the dark nodes are the classical vertices of this free knot and the simple crossings are the virtual crossings (since there are many virtual crossings we deemed this change of convention necessary). We show that the  $G_2$  bracket detects the non-triviality of  $G$  by exhibiting a state that survives in the invariant

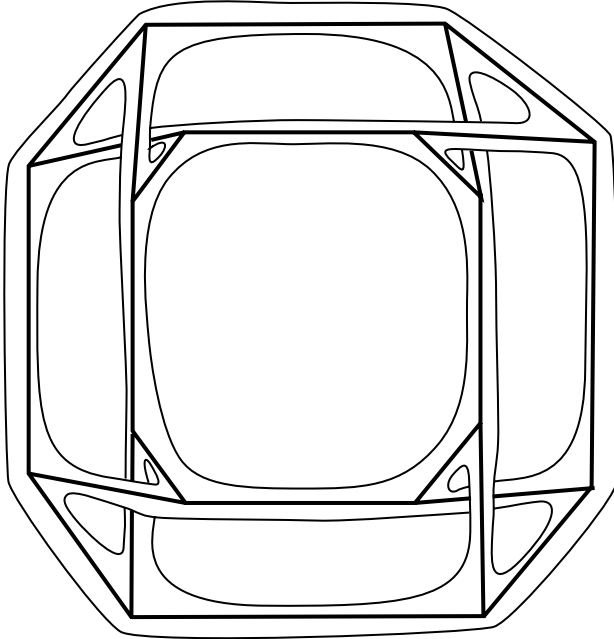


Fig. 39. A surface for the state of the flat link  $L$ .

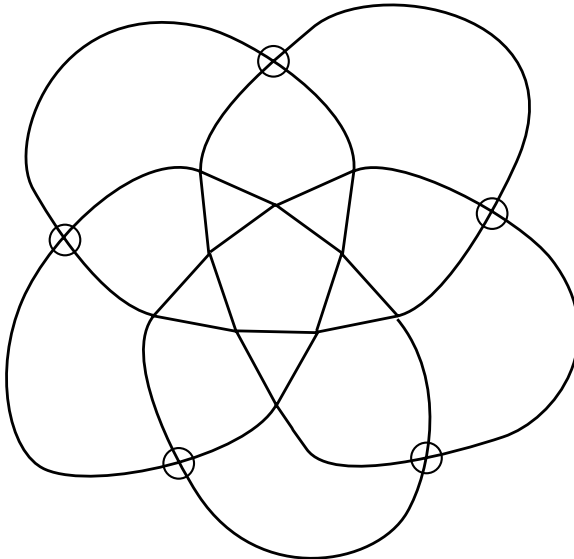


Fig. 40. Possibly irreducible but undetectable by  $G_2$  invariant.

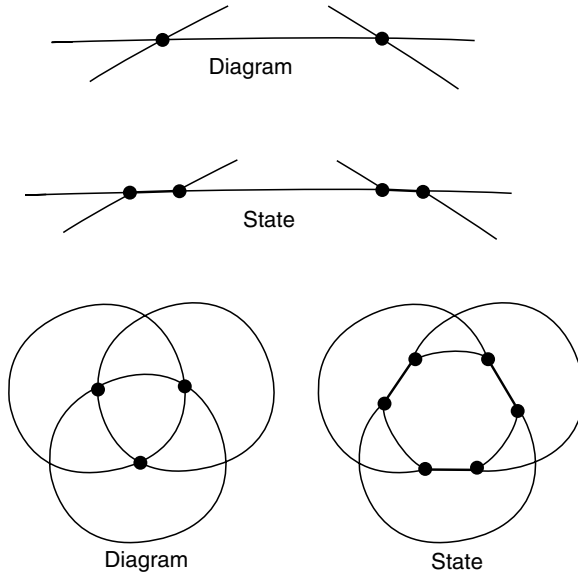


Fig. 41. Diagram and state.

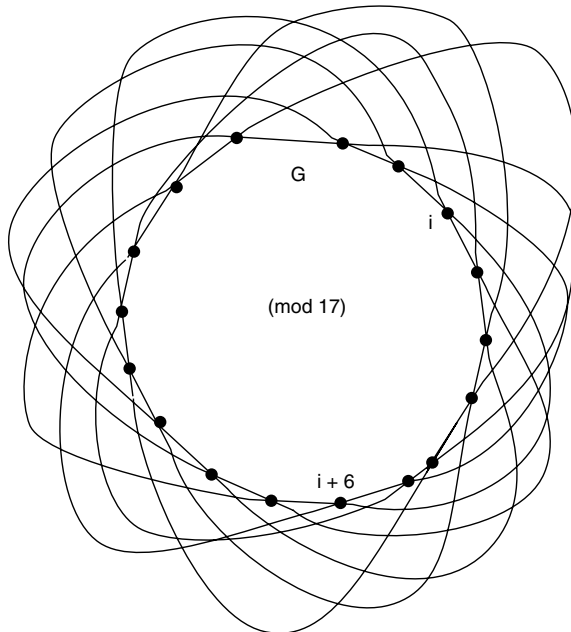


Fig. 42. A non-trivial free knot  $G$ .

and is irreducible. The state is constructed in analogy with the state construction shown in Fig. 41. In Fig. 41 a typical pair of adjacent classical vertices and the corresponding  $G_2$  state. We illustrate this in Fig. 41 for a circle of three vertices and ask the reader to consider the same pattern for the 17 vertices of  $G$  in Fig. 42. It is then apparent to inspect that  $G$  has no cycles (just as a graph with no restrictions on framing at crossings) of small length (2, 3, 4 or 5) and that the same is true for the corresponding state  $S$  of  $G$ . Thus  $S$  is irreducible and it is easy to see that  $S$  appears with non-zero coefficient in the  $G_2$  invariant of  $G$ , since any irreducible state with a maximal number of paired trivalent replacements has positive coefficient in the invariant. This completes the proof that  $G$  is non-trivial.

We should further remark that there is a special state that can be constructed from a free knot  $L$ . This state is the one where crossings are replaced by pairs of trivalent vertices such that the resulting state graph is bipartite. Call this state  $B(L)$ . The reader will be interested to find examples of free knots that are distinguished by their bipartite state.

### 7. On the Penrose Coloring Bracket

A *proper edge 3-coloring* of a trivalent graph is an assignment of three colors (say from the set  $\{0, 1, 2\}$ ) to the edges of the graph such that three distinct colors appear at every vertex. In [32] Penrose gives a bracket that counts the proper edge 3-colorings of a trivalent plane graph.

The Penrose bracket [32] is defined as shown in Fig. 43. Penrose devised this bracket and other combinatorial expansions based on abstract tensors. In the case

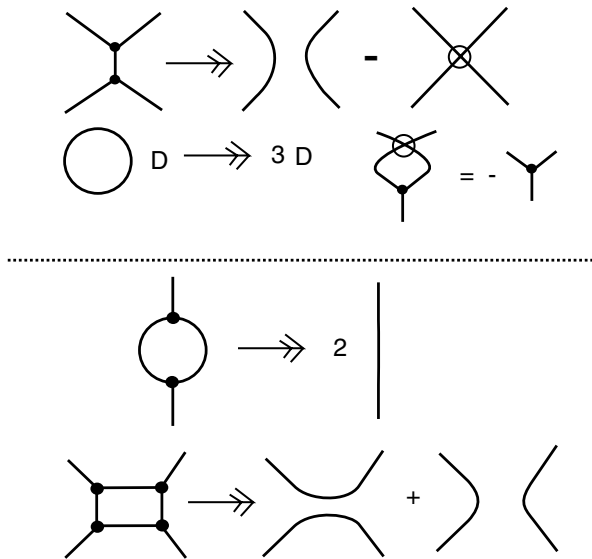


Fig. 43. Penrose bracket and identities.

of this Penrose bracket, we will show that it is a special case of the Kuperberg  $sl(3)$  bracket and explain how flat virtual knots are related to classical graph coloring problems.

The Penrose bracket is an evaluation of trivalent graphs immersed in the plane so that cyclic orders at the nodes are given. It can be defined independently of the planar immersion as long as the cyclic orders at the nodes are specified, but counts colorings correctly only for planar *embeddings*. Thus the Penrose bracket is well-defined for virtual graphs (see Definition 2) as we have defined them earlier in the paper. Note that in the expansion formula for the Penrose bracket we have one term with crossed lines and a virtual crossing. In completely expanding a graph by this formula one has many curves with virtual self-crossings. Each curve is evaluated as the number 3 and thus the evaluation of the Penrose bracket is a signed sum of powers of 3.

Note in Fig. 43 the identities that we have listed. These follow from the expansion formulas above the line. It is then apparent that the evaluation of the Kuperberg  $sl(3)$  bracket at  $A = 1$  on an oriented trivalent plane graph is equal to the value of the Penrose bracket for this graph. The Kuperberg bracket is calculated by the same reduction formulas as the Penrose bracket, and for the oriented graph, we only need the bigon and quadrilateral reductions. This observation is the main reason we mention the Penrose bracket in this context.

In Fig. 44 we show the other reduction identities for the Penrose bracket (for triangles, pendant loops and five-sided regions). These identities can be used to evaluate the Penrose bracket for unoriented plane graphs, since an Euler characteristic argument tells us that any trivalent graph in the plane with no isthmus must have a region with less than six sides. We can take the reduction formalism of the Penrose bracket and attempt to use it to create new invariants of free knots. This will be the subject of a separate paper.

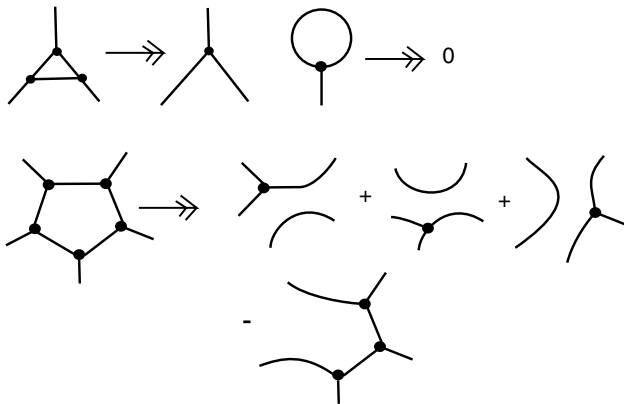


Fig. 44. Further Penrose bracket identities.

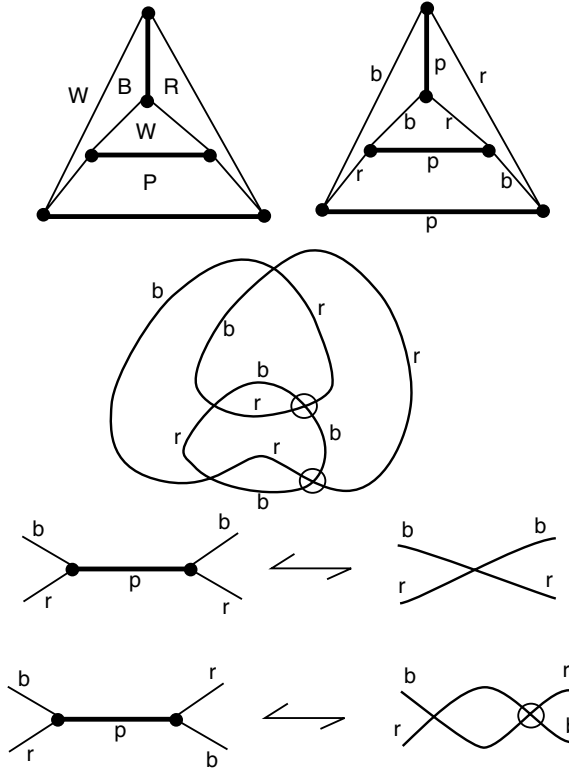


Fig. 45. Coloring graphs and free knots.

Finally, we point out a relationship between coloring maps, graphs and free knots and links. Examine Fig. 45. At the top left of the figure we show a trivalent graph in the plane with a 4-coloring of its regions by the colors  $\{W, R, B, P\}$ . Two regions that share an edge are colored with different colors. This graph is a simplest example of a plane graph that requires four colors. Adjacent to the coloring of the regions of this graph we have illustrated a coloring of its edges by the three colors  $\{r, b, p\}$  so that every node of the graph has three distinct colored edges incident to it. The edge coloring can be obtained from the face coloring by regarding  $\{W, R, B, P\}$  as isomorphic to the group  $\mathbb{Z}_2 \times \mathbb{Z}_2$  with  $W$  the identity element and  $R^2 = B^2 = P^2 = W$  and  $RB = BR = P, RP = PR = B, BP = PB = R$ . Then the edge coloring is obtained by coloring each edge with the product of the region colors on either side of it.

**Definition 9.** Call a component in a free link diagram (represented as a planar diagram) *even* if there are an even number of virtual crossings on this component that occur between the given component and other components of the link. (See Sec. 2.3 for definitions related to framed and free knots and links.) Call a free link

diagram *componentwise even* if every component of the link is even. Note that a single component free knot diagram is componentwise even since there are zero virtual crossings between the one component and any other component.

In the right-hand side of Fig. 45 we illustrate a free link diagram that is obtained from the edge-colored graph above it by using the translations illustrated below the free link diagram. In these translations we use two colors for the edges of a free link. *Opposite edges are colored by different colors from the binary set  $\{r, b\}$ .*

**Definition 10.** We call a free link diagram *2-colored* if it is colored in  $\{r, b\}$  so that opposite edges have different colors. It is clear from the definition that *a free link diagram can be 2-colored if and only if it is componentwise even.*

By using the translations in the figure we see that *an edge-colored trivalent graph immersed in the plane corresponds uniquely to a colored free link diagram.* In the figure we see that a colored planar graph may correspond to a free link diagram that has virtual crossings. The relationship between planar colorings and properties of free links needs further study.

### 8. Remarks

This paper arose through our discussions of new possibilities in virtual knot theory and in relation to advances of Manturov using parity in virtual knot theory, particularly in the area of free knots. In the paper [30], there is a model for the  $sl(n)$ -version of the Homflypt polynomial for classical knots. This model is based on patterns of smoothings as shown in Fig. 46.

These patterns suggested to us the techniques we use in this paper with the Kuperberg brackets, and we expect to generalize them further. In this method, the value of the polynomial for a knot is equal to the linear combination of the values for two graphs obtained from the knot by resolving the two crossings as shown in Fig. 46.

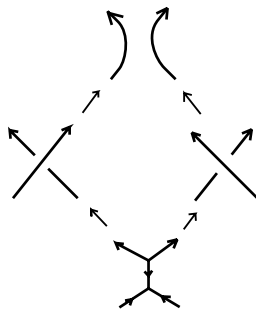


Fig. 46. Murakami–Ohtsuki–Yamada relation for  $sl(n)$ .

**Note.** The following references [1, 7, 8, 15, 16, 21, 25, 31] will, along with the other references cited in the text of the paper, be useful to the reader for background matters.

## Acknowledgments

We would like to take this opportunity to thank the Mathematisches Forschungsinstitut Oberwolfach for their hospitality and wonderful research atmosphere. A first paper on this subject was written at the MFO in June 2012 at a Research in Pairs of the present authors. The present paper was completed at the MFO in June 2014 at a second Research in Pairs of the authors. The second named author was partially supported by Laboratory of Quantum Topology of Chelyabinsk State University (Russian Federation government grant 14.Z50.31.0020) and by grants of the Russian Foundation for Basic Research, 13-01-00830, 14-01-91161, 14-01-31288.

## References

- [1] J. S. Carter, S. Kamada and M. Saito, Stable equivalences of knots on surfaces and virtual knot cobordisms, *J. Knot Theory Ramifications* **11**(3) (2002) 311–322.
- [2] H. A. Dye and L. H. Kauffman, Virtual crossing number and the arrow polynomial, *J. Knot Theory Ramifications* **18**(10) (2009) 1335–1357.
- [3] M. Goussarov, M. Polyak and O. Viro, Finite type invariants of classical and virtual knots, *Topology* **39** (2000) 1045–1068.
- [4] J. Hass and P. Scott, Shortening curves on surfaces, *Topology* **33**(1) (1994) 25–43.
- [5] D. P. Ilyutko, V. O. Manturov and I. M. Nikonov, Virtual knot invariants arising from parities, preprint (2011), arXiv:1102.5081.
- [6] T. Kadokami, Detecting non-triviality of virtual links, *J. Knot Theory Ramifications* **12**(6) (2003) 781–803.
- [7] N. Kamada and S. Kamada, Abstract link diagrams and virtual knots, *J. Knot Theory Ramifications* **9**(1) (2000) 93–106.
- [8] L. H. Kauffman, *Knots and Physics* (World Scientific, 1991); 2nd edn. (1993); 3rd edn. (2002); 4th edn. (2012).
- [9] L. H. Kauffman, Virtual knot theory, *European J. Combin.* **20** (1999) 663–690.
- [10] L. H. Kauffman, A survey of virtual knot theory, in *Proc. Knots in Hellas '98* (World Scientific, 2000), pp. 143–202.
- [11] L. H. Kauffman, Detecting virtual knots, *Atti. Sem. Mat. Fis. Univ. Modena* **49**(Suppl.) (2001) 241–282.
- [12] L. H. Kauffman, A self-linking invariant of virtual knots, *Fund. Math.* **184** (2004) 135–158.
- [13] L. H. Kauffman, Knot diagrammatics, in *Handbook of Knot Theory*, eds. W. Menasco and M. Thistlethwaite (Elsevier B. V., Amsterdam, 2005), pp. 233–318.
- [14] L. H. Kauffman, An extended bracket polynomial for virtual knots and links, *J. Knot Theory Ramifications* **18**(10) (2009) 1369–1422.
- [15] L. H. Kauffman, R. A. Fenn and V. O. Manturov, Virtual knot theory — Unsolved problems, *Fund. Math.* **188** (2005) 293–323.
- [16] L. H. Kauffman and S. Lambropoulou, A categorical structure for the virtual braid group, *Comm. Algebra* **39**(12) (2011) 4679–4704.



- [17] L. H. Kauffman and V. O. Manturov, A graphical construction of the  $sl(3)$  invariant for virtual knots, *Quantum Topol.* **5**(4) (2014) 523–539.
- [18] V. A. Krasnov and V. O. Manturov, Graph-valued invariants of virtual and classical links and minimality problem, *J. Knot Theory Ramifications* **22**(12) (2013), Article ID: 1341006, 14pp.
- [19] G. Kuperberg, The quantum  $G_2$  link invariant, *Internat. J. Math.* **5** (1994) 61–85.
- [20] G. Kuperberg, What is a virtual link? *Algebr. Geom. Topol.* **3** (2003) 587–591 (electronic).
- [21] V. O. Manturov, Khovanov homology of virtual knots with arbitrary coefficients, *Izve. Math.* **71**(5) (2007) 967–999; *Izv. RAN. Ser. Mat.* **71**(5) (2007) 111–148 (in Russian); *J. Knot Theory Ramifications* **16**(3) (2007) 345–377.
- [22] V. O. Manturov, On free knots, preprint (2009), arXiv:0901.2214.
- [23] V. O. Manturov, Parity in knot theory, *Math. Sb.* **201**(5) (2010) 65–110.
- [24] V. O. Manturov, Parity in knot theory, *Math. Sb.* **201**(5) (2010) 693–733.
- [25] V. O. Manturov, Free knots and parity, in *Proc. Advanced Summer School on Knot Theory with its Applications to Physics and Biology*, Trieste, May 11–29, 2009, Series on Knots and Everything, Vol. 46 (World Scientific, 2011), pp. 321–345.
- [26] V. O. Manturov, On virtual crossing numbers of virtual knots, *J. Knot Theory Ramifications* **21** (2012), Article ID: 1240009, 13pp.
- [27] V. O. Manturov, Parity and projection from virtual knots to classical knots, *J. Knot Theory Ramifications* **22**(9) (2013), Article ID: 1350044, 20pp.
- [28] V. O. Manturov, Almost complete classification of free links, *Dokl. Math.* **88**(2) (2013) 1–3.
- [29] V. O. Manturov and D. Ilyutko, *Virtual Knots: The State of the Art* (World Scientific, 2012).
- [30] H. Murakami, T. Ohtsuki and S. Yamada, Homflypt polynomial via an invariant of colored planar graphs, *Enseign. Math.* **44** (1988) 325–360.
- [31] T. Ohtsuki, *Quantum Invariants*, Series on Knots and Everything, Vol. 29 (World Scientific, 2002).
- [32] R. Penrose, Applications of negative dimensional tensors, in *Combinatorial Mathematics and its Applications*, ed. D. J. A. Welsh (Academic Press, 1971), pp. 221–244.
- [33] K. Reidemeister, *Knotentheorie* (Chelsea Publishing, 1948).
- [34] V. G. Turaev, Virtual strings, *Ann. Inst. Fourier (Grenoble)* **54**(7) (2004) 2455–2525.
- [35] V. G. Turaev, Topology of words, *Proc. Lond. Math. Soc. (3)* **95**(2) (2007) 360–412.